

Multistability and regime shifts in microbial communities explained by competition for essential nutrients

Veronika Dubinkina*

*Department of Bioengineering and Carl R. Woese Institute for Genomic Biology,
University of Illinois at Urbana-Champaign, Urbana, IL 61801, USA*

Yulia Fridman*

*National Research Center "Kurchatov Institute",
Akademika Kurchatova pl., Moscow, 123182, Russia*

Parth Pratim Pandey*

*Carl R. Woese Institute for Genomic Biology and National Center for Supercomputing Applications,
University of Illinois at Urbana-Champaign, Urbana, IL 61801, USA*

Sergei Maslov[†]

*Department of Bioengineering and Carl R. Woese Institute for Genomic Biology,
University of Illinois at Urbana-Champaign, Urbana, IL 61801, USA.*

(Dated: August 10, 2021)

Microbial communities routinely have several possible species compositions or community states observed for the same environmental parameters. Changes in these parameters can trigger abrupt and persistent transitions (regime shifts) between such community states. Yet little is known about the main determinants and mechanisms of multistability in microbial communities. Here we introduce and study a resource-explicit model in which microbes compete for two types of essential nutrients. We adapt game-theoretical methods of the stable matching problem to identify all possible species compositions of a microbial community. We then classify them by their resilience against three types of perturbations: fluctuations in nutrient supply, invasions by new species, and small changes of abundances of existing ones. We observe multistability and explore an intricate network of regime shifts between stable states in our model. Our results suggest that multistability requires microbial species to have different stoichiometries of essential nutrients. We also find that balanced nutrient supply promote multistability and species diversity yet make individual community states less stable.

INTRODUCTION

Recent metagenomics studies revealed that microbial communities collected in similar environments are often composed of rather different sets of species^{1–6}. It remains unclear to what extent such alternative species compositions are deterministic as opposed to being an unpredictable outcome of communities' stochastic assembly. Furthermore, changes in environmental parameters may trigger abrupt and persistent transitions between these alternative species compositions^{7–9}. Such transitions, known as ecosystem regime shifts, significantly alter the function of a microbial community and are difficult to reverse. Understanding mechanisms and principal determinants of alternative species compositions and shifts between them is practically important. Thus they have been extensively studied over the past several decades^{10–16}.

Growth of microbial species is affected by many factors, with availability of nutrients being among the most important ones. Thus the supply of nutrients and competition for them plays a crucial role in determining the species composition of a microbial community. The majority of modeling approaches explicitly taking nutrients into account are based on the classic MacArthur

consumer-resource model and its variants^{17–24}. This model assumes that every species co-utilizes several perfectly substitutable nutrients of a single type (e.g. carbon sources). However, it is well known that nutrients required for growth of a species exist in the form of several essential (non-substitutable) types including sources of C, N, P, Fe, etc. While real-life ecosystems driven by competition for multiple essential nutrients have been studied experimentally^{25–27}, the resource-explicit models capturing this type of growth are not so well developed beyond the foundational work by Tilman²⁸.

Here we introduce and study a new resource-explicit model of a microbial community supplied with multiple metabolites of two essential types. This ecosystem is populated by microbes selected from a fixed pool of species. We show that our model has a very large number of possible steady states classified by their species compositions. Using game-theoretical methods adapted from the well-known stable marriage problem^{29,30}, we predict all of these states based only on the ranked lists of competitive abilities of individual species for each of the nutrients. We further classify these states by their dynamic stability, and whether they could be invaded by other species in our pool. We then focus our attention on a set of steady states that are both dynamically stable and

resilient with respect to species invasion.

For each state we identify its feasibility range of all possible environmental parameters (nutrient supply rates) for which all of state's species are able to survive. We further demonstrate that for a given set of nutrient supply rates, more than one state could be simultaneously feasible, thereby allowing for multistability. While the overall number of stable states in our model is exponentially large, only very few of them can be realized for a given set of environmental conditions quantified by nutrient supply rates. The principal component analysis of predicted microbial abundances in our model shows a separation between the alternative stable states reminiscent of real-life microbial ecosystems. We further explore an intricate network of regime shifts between the alternative stable states in our model triggered by changes in nutrient supply. Our results suggest that multistability requires microbial species to have different stoichiometries of two essential resources. We also find that well-balanced nutrient supply rates matching the average species' stoichiometry promote multistability and species diversity yet make individual community states less structurally and dynamically stable. These and other insights from our resource-explicit model may help to understand the existing data and provide guidance for future experimental studies of alternative stable states and regime shifts in microbial communities.

I. RESULTS

A. Microbial community growing on two types of essential nutrients represented by multiple metabolites

Our resource-explicit model describes a microbial ecosystem colonized by microbes selected from a pool of S species. Growth of each of these species could be limited by two types of essential resources, to which we refer to as "carbon" and "nitrogen". In principle, these could be any pair of resources essential for life: C, N, P, Fe, etc. A generalization of this model to more than two types of essential resources (e.g. C, N and P) is straightforward. Carbon and nitrogen resources exist in the environment in the form of K distinct metabolites containing carbon, and M other metabolites containing nitrogen. For simplicity we ignore the possibility of the same metabolite providing both types. We further assume that each of the S species in the pool is a specialist, capable of utilizing only a single pair of nutrients, i.e., one metabolite containing carbon and one metabolite containing nitrogen.

We assume that for given environmental concentrations of all nutrients, a growth rate of a species α is limited by a single essential resource via Liebig's law of the minimum³¹:

$$g_\alpha(c, n) = \min(\lambda_\alpha^{(c)}c, \lambda_\alpha^{(n)}n) \quad . \quad (1)$$

Here c and n are the environmental concentrations of

unique carbon and nitrogen resources consumed by this species. The coefficients $\lambda_\alpha^{(c)}$ and $\lambda_\alpha^{(n)}$ are defined as species-specific growth rates per unit of concentration of each of two resources. They quantify the competitive abilities of the species α for its carbon and nitrogen resources, respectively. Indeed, according to the competitive exclusion principle, if two species are limited by the same resource, the one with the larger value of λ wins the competition. Note that according to Liebig's law, if the carbon source is in a short supply so that $\lambda_\alpha^{(c)}c < \lambda_\alpha^{(n)}n$, it sets the value for this species growth rate. We refer to this situation as *c-source limiting* the growth of species α . Conversely, when $\lambda_\alpha^{(c)}c > \lambda_\alpha^{(n)}n$, the *n-source is limiting* the growth of this species. Thus each species always has exactly one growth-limiting resource and one non-limiting resource.

In our model microbes grow in a well-mixed chemostat-like environment subject to a constant dilution rate δ (see Fig. 1A for an illustration). The dynamics of the population density, B_α , of a microbial species α is then governed by:

$$\frac{dB_\alpha}{dt} = B_\alpha [g_\alpha(c_i, n_j) - \delta] \quad , \quad (2)$$

where c_i and n_j are the specific pair of nutrients defining the growth rate g_α of this species according to the Liebig's law (Eq. 1). These nutrients are externally supplied at fixed rates $\phi_i^{(c)}$ and $\phi_j^{(n)}$ and their concentrations follow the equations:

$$\begin{aligned} \frac{dc_i}{dt} &= \phi_i^{(c)} - \delta \cdot c_i - \sum_{\text{all } \alpha \text{ using } c_i} B_\alpha \frac{g_\alpha(c_i, n_j)}{Y_\alpha^{(c)}} \quad , \\ \frac{dn_j}{dt} &= \phi_j^{(n)} - \delta \cdot n_j - \sum_{\text{all } \alpha \text{ using } n_j} B_\alpha \frac{g_\alpha(c_i, n_j)}{Y_\alpha^{(n)}} \quad . \end{aligned} \quad (3)$$

Here $Y_\alpha^{(c)}$ and $Y_\alpha^{(n)}$ are the growth yields of the species α on its *c*- and *n*-resources respectively. Yields quantify the concentration of microbial cells generated per unit of concentration of each of these two consumed resources. The yield ratio $Y_\alpha^{(n)}/Y_\alpha^{(c)}$ determines the unique C:N stoichiometry of each species.

A steady state of the microbial ecosystem can be found by setting the right hand sides of Eqs 2-3 to zero and solving them for environmental concentrations of all nutrients c_i , and n_j , and abundances B_α of all species. We choose to label all possible steady states by the list of species present in the state and *by the growth-limiting nutrient (c or n) for each of these species*. Thus, two identical sets of species, where at least one species is growth limited by a different nutrient are treated as two distinct states of our model. Conversely, our definition of a steady state does not take into account species' abundances. Examples of such states in a system with 2 carbon, 2 nitrogen nutrients and 4 species (one species for every pair of carbon and nitrogen nutrients) with specific values of species' competitive abilities $\lambda_\alpha^{(c)}$ and $\lambda_\alpha^{(n)}$ and yields $Y_\alpha^{(c)}$

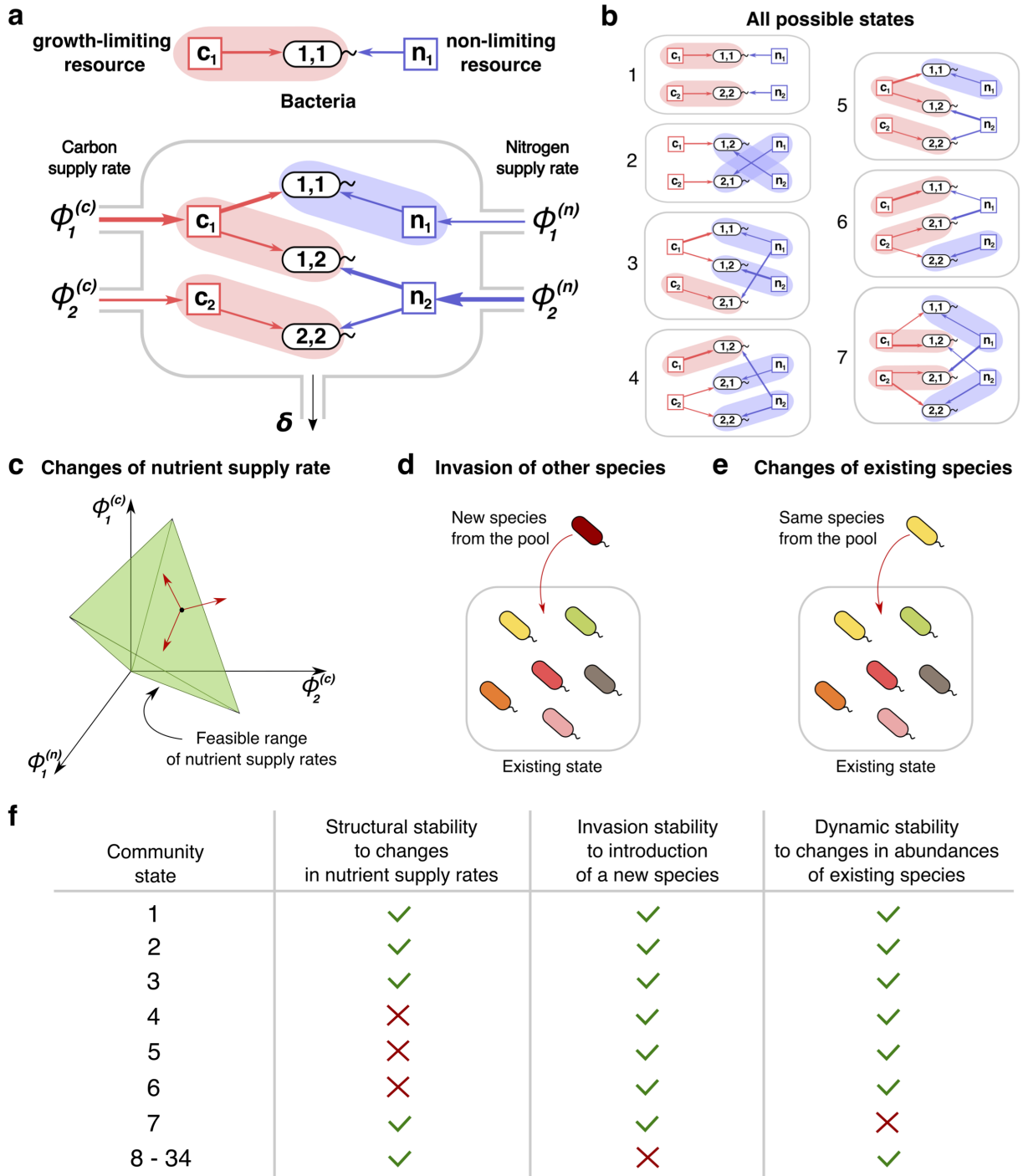


FIG. 1. Community states and different types of their stability. (a) A schematic depiction of the proposed experimental setup and one of several possible community states in the $2C \times 2N \times 4S$ model. Several sources of carbon and nitrogen are supplied at constant rates $\phi_i^{(c)}$ and $\phi_j^{(n)}$ to a chemostat with a dilution rate δ . Red and blue square nodes represent these nutrients inside the chemostat with steady state concentrations c_1, c_2 (for carbon) and n_1, n_2 (for nitrogen). They are consumed by three microbial species labeled by the pair of carbon (the first index) and nitrogen (the second index) nutrients this species consumes. Shaded ovals connect every species to its unique growth-limiting nutrients. The fourth species 2, 1 is not present in this steady state. (b) All 7 uninvadable states in the $2C \times 2N \times 4S$ model are depicted using the same schematic representation as in (a). Panels (c-e) schematically depict the three possible types of perturbations of a community state, corresponding to three different types of its stability. (c) Changes of nutrient supply rates, that may result in extinction of some of the species. Green shaded area schematically depicts the region of nutrient supply rates where a given state is feasible, red arrows represent the perturbations of nutrient supply rates. (d) Introduction of species currently absent from the system, i.e. invasion, that may change the set of surviving species. (e) Small fluctuations in abundances of existing species, that may disturb the dynamic equilibrium of the system and potentially drive it to another state. (f) Table that shows which stability criteria are satisfied for 34 possible states of the $2C \times 2N \times 4S$ model. Note that these types of stability are in general unrelated to each other.

and $Y_\alpha^{(n)}$ (see Supplementary Tables 1,2 for their exact values) are shown in Fig. 1B. For the sake of brevity we refer to this model as $2C \times 2N \times 4S$.

Because each of the S species in the pool could be absent from a given state, or, if present, could be limited by either its c - or its n -resource, the theoretical maximum of the number of distinct states is 3^S (equal to 81 in our $2C \times 2N \times 4S$ example). However, the actual number of possible steady states is considerably smaller (equal to 34 in this case). Indeed, possible steady states in our model are constrained by a variant of the competitive exclusion principle³² (see Methods for details). One of the universal consequences of this principle is that the number of species present in a steady state of any consumer-resource model cannot exceed $K + M$ - the total number of nutrients. We greatly simplified the task of finding all steady states in our model by the discovery of the exact correspondence between our system and a variant of the celebrated stable matching (or stable marriage) problem in game theory and economics^{29,30}. (see Methods and Supplementary Materials, section).

Three criteria for stability of microbial communities

Each of the steady states identified in the previous chapter can be realized only for a certain range of nutrient supply rates. These ranges can be calculated using the steady state solutions of Eqs. 2, 3, governing the dynamics of microbial populations and nutrient concentrations respectively (see Methods). Among all formal mathematical solutions of these equations we select those where populations of all species and all nutrient concentrations are non-negative. This imposes constraints on nutrient supply rates, thereby determining their feasible range for a given steady state (shown in green in Fig. 1C). The volume of such feasible range has been previously used to quantify the so-called structural stability of a steady state^{24,33,34}. States with larger feasible volumes generally tend to be more resilient with respect to fluctuations in nutrient supply.

Stability of a community steady state could be also disturbed by a successful invasion of a new species (see Fig. 1D). We can test the resilience of a given state in our model with respect to invasions by other species. A state is called uninvadable if none of the other species from our pool can survive in the environment shaped by the existing species.

In addition to structural and invasion types of stability described above, there is also a notion of dynamic stability of a steady state actively discussed in the ecosystems literature (see e.g.^{24,35,36}). Dynamic stability can be tested by exposing a steady state to small perturbations in populations of all species present in this state (see Fig. 1E). The state is declared dynamically stable if after any such disturbance the system ultimately returns to its initial configuration (see Methods for details of the testing procedure used in our study).

We classify all of the steady states in our model according to these three types of stability. The example of this classification for the $2C \times 2N \times 4S$ model is summarized in Fig. 1F. Note, that in general, one type of stability does not imply another. Out of 34 possible steady states realized for different ranges of nutrient supply rates there are only 7 uninvadable ones. Unlike other consumer resource models, in our model the dynamic stability of a state with respect to species invasions does not depend on nutrient supply rates. In the $2C \times 2N \times 4S$ model only one of the states (labelled 7 in Fig. 1B) turned out to be dynamically unstable, while for the remaining 33 states small perturbations of microbial abundances present in the state did not trigger a change of the state. Unlike two other types of stability, the structural stability has a continuous range. It could be quantified by the fraction of all possible combinations of nutrient supply rates for which a given state is feasible (referred to as state's normalized feasible range). We estimated normalized feasible ranges of all states in the $2C \times 2N \times 4S$ model using a Monte Carlo procedure described in Methods. The results are reflected in the second column of Fig. 1F, where a structurally stable state is defined as that whose normalized feasible range exceeds 0.1. In general we find that normalized feasible ranges of uninvadable states in our model have a broad log-normal distribution (see Fig. S2 for details).

It is natural to focus our attention on steady states that are simultaneously uninvadable and dynamically stable. Indeed, such states correspond to natural endpoints of the microbial community assembly process. They would persist for as long as the nutrient supply rates do not change outside of their structural stability range. Therefore, they represent the states of microbial ecosystems that are likely to be experimentally observed. From now on we concentrate our study almost exclusively on those states and refer to them simply as stable states.

B. Regime shifts between alternative stable states

The feasible ranges of nutrient supply of different stable states may or may not overlap with each other (see Fig. 2A-B for a schematic illustration of two different scenarios). Whenever feasible ranges of two or more states overlap (see Fig. 2B) - multistability ensues. Note that the states in the overlapping region of their feasibility ranges constitute true alternative stable states defined and studied in the ecosystems literature^{10-12,15,16}. The existence of alternative stable states goes hand-in-hand with regime shifts manifesting themselves as large discontinuous and hysteretic changes of species abundances⁹. Every pair of states with overlapping feasibility ranges in our model corresponds to a possible regime shift between these states illustrated in Fig. 2D (note discontinuous changes in population B_{11} of the microbial species (1, 1) at the boundaries of the overlapping region). Conversely, when feasible ranges of a pair of states do not

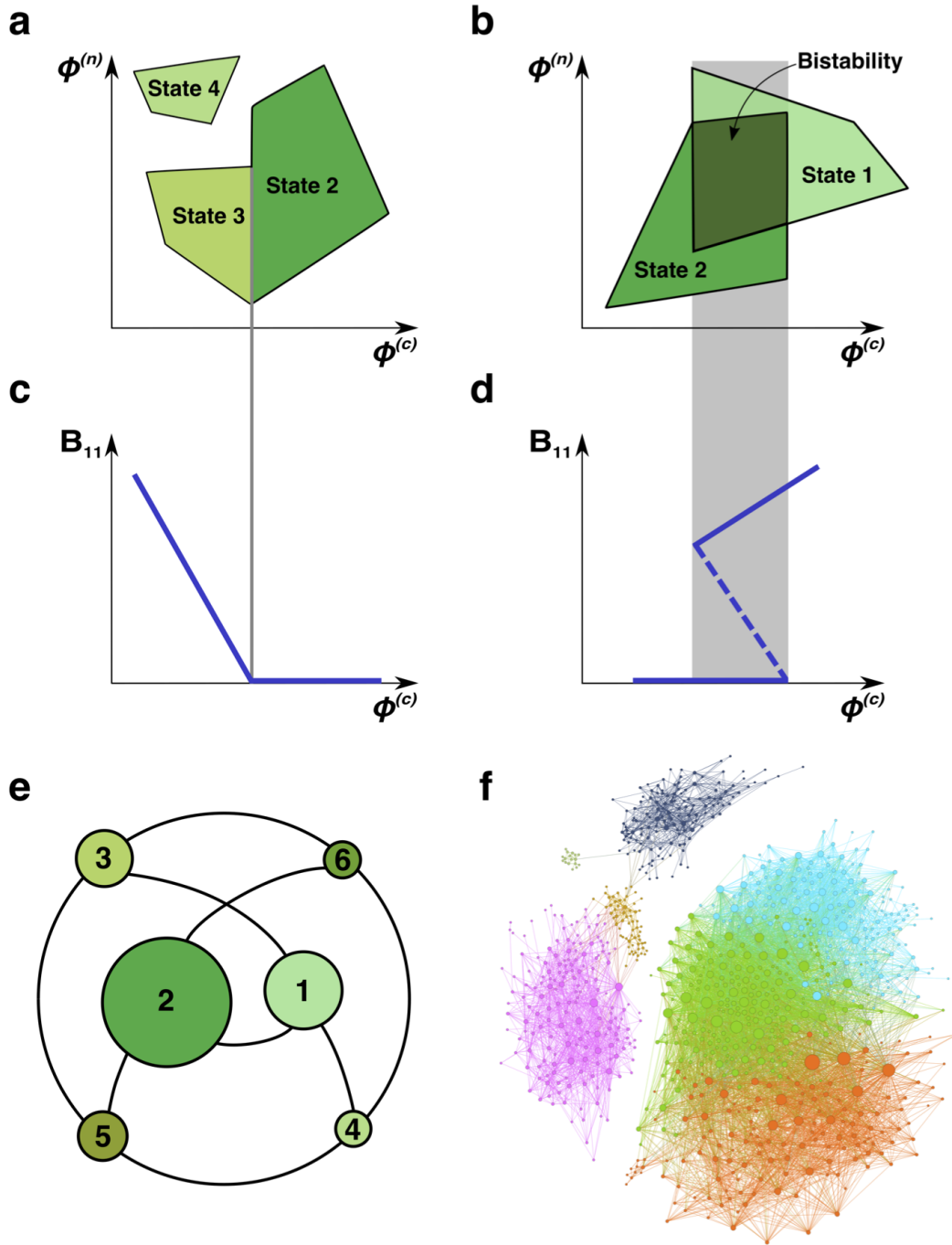


FIG. 2. **Regime shifts between alternative stable states.** (a) Shaded green areas schematically depict the feasible ranges of nutrient supply rates for several stable states in our model (#2-#4 in Fig. 1B). The feasible range of the state #4 does not overlap with that of any other state. Feasible ranges of states #2 and #3 also do not overlap but share a common boundary. Panel (b) depicts the opposite scenario of overlapping feasible ranges of another pair of stable states (#1 and #2 in Fig. 1B). In the overlapping region (dark green) they form a pair of alternative stable states. (c) A smooth transition between two states at the boundary. The population B_{11} of the microbial species (1, 1) is plotted as a function of changing nutrient supply rate $\phi^{(c)}$ (same as the x-axis in panel (a)). Vertical gray line corresponds to the boundary between states #3 and #2. (d) A regime shift between two states. B_{11} is plotted as a function of nutrient supply $\phi^{(c)}$ as it sweeps through the overlapping region (gray area) in panel (b). Note abrupt changes of B_{11} at the boundaries of the overlapping region and its hysteretic behavior as expected for regime shifts. Dashed line corresponds to B_{11} in a dynamically unstable state (#7 in Fig. 1B). (e) The network of possible regime shifts between pairs of stable states in the $2C \times 2N \times 4S$ model. Each link represents a possible regime shift between two states it connects (overlap of their feasible ranges), nodes correspond to 6 uninvadable and dynamically stable states (state labels are the same as in Fig. 1B). Sizes of nodes reflect relative magnitudes of feasible ranges of states they represent. (f) Network of 8633 possible regime shifts between pairs of 893 uninvadable dynamically stable states in the $6C \times 6N \times 36S$ model. The size of each node reflects its degree (i.e. the total number of other stable states that a given state can shift into). The color of each node corresponds to its network modularity class calculated as described in Methods.

overlap with each other but instead share a boundary (Fig. 2A), the transition between these states is smooth and non-hysteretic (Fig. 2C). It manifests itself in continuous changes in abundances of all microbial species at the boundary between states.

As expected for regime shifts, dynamically unstable states always accompany multistable regions in our model⁹ (see below for the detailed discussion of the interplay between multistability and dynamically unstable states). We observed that dynamically unstable state 7 in our $2C \times 2N \times 4S$ is feasible in the overlapping region between states 1 and 2 in Fig. 2B. The population B_{11} in this state is shown as dashed line in Fig. 2D.

We identified all possible regime shifts in the $2C \times 2N \times 4S$ model by systematically looking for overlaps between feasible ranges of nutrient supply of all six uninvadable dynamically stable states. These regime shifts can be represented as a network in which nodes correspond to community's stable states and edges connect states with partially overlapping feasible ranges (see Fig. 2E). Note that in general, this network does not capture overlaps between feasible ranges of more than two stable states, which will be discussed in the next section. Fig. 2F shows a much larger network of 8633 regime shifts between 893 uninvadable dynamically stable states in the $6C \times 6N \times 36S$ variant of our model. In this model the microbial community is supplied with 6 carbon and 6 nitrogen nutrients and colonized from a pool of 36 microbial species (one for each pair of C and N nutrients) (see Supplementary Tables III, IV, V, VI for the values of λ 's and yields). For simplicity we did not show the remaining 165 uninvadable stable states that have no possible regimes shifts to any other states. The size of a node is proportional to its degree (i.e. the total number of other states it overlaps with) ranging between 1 and 164 with average around 20 (degree distribution is shown in Fig. S3). The network modularity analysis (see Methods for details) revealed 7 network modules indicating that pairs of states that could possibly undergo a regime shift are clustered together in the multi-dimensional space of nutrient supply rates.

C. Patterns of multistability

In a general case, the number of stable states that are simultaneously feasible for given nutrient supply rates can be more than two. Furthermore, as the number of nutrients increases, the multistability with more than two stable states becomes progressively more common. In Fig. 3A we quantify the frequency with which V multistable states occur in our $6C \times 6N \times 36S$ model across all possible nutrient supply rates (see Methods for details of how this was estimated). $V - 1$ approximately follows a Poisson distribution (dashed line in Fig. 3A) with $\lambda = 0.063$. Note that for some supply rates up to 5 stable states can be simultaneously feasible. However, the probability to find such cases is exponentially small.

We further explored the factors that determine whether multistability is possible in resource-limited microbial communities and if yes, how common it is among different nutrient supply rates. Like in a simple special case of regime shift between two microbial species studied in Ref.²⁸, multistability in our model is only possible if individual microbial species have different C:N stoichiometry. This stoichiometry is given by the ratio of species' nitrogen and carbon yields. Our numerical simulations and mathematical arguments (see Supplementary Material, section) show that when all species have exactly the same stoichiometry $Y_\alpha^{(n)}/Y_\alpha^{(c)}$, there is no multistability or dynamical instability in our model. That is to say, in this case for every set of nutrient supply rates the community has a unique uninvadable state, and all these states are dynamically stable. Simulations of the $2C \times 2N \times 4S$ example (see Fig. S4) show that the more similar is species' C:N stoichiometry (quantified by stan-

dard deviation of $\frac{Y_{ij}^{(n)}}{Y_{ij}^{(c)}}$), the less likely it is to find multistability among all possible nutrient supply rates (see Fig. S4).

A complementary question is whether multistable states are more common around particular ratios of carbon and nitrogen supply rates. Fig. 3B shows this to be the case: the likelihood of multistability has a sharp peak around the well-balanced C:N nutrient supply rates. In this region multiple stable states are present for roughly 15% of nutrient supply rate combinations. Note that the average C:N stoichiometry of species in our model is assumed to be 1:1. In a more general case, the peak of multistability is expected to be close to the average C:N stoichiometry of species in the community.

To illustrate how multistable states manifest themselves in a commonly performed Principle Component Analysis (PCA) of species' relative abundances, we picked the environment with $V = 5$ simultaneously feasible stable states in our $6C \times 6N \times 36S$ model. In natural environments nutrient supply usually fluctuates both in time and space. To simulate this we sampled a $\pm 10\%$ range of nutrient supply rates around this chosen environment (see Methods) and calculated species' relative abundances in each of the uninvadable states feasible for a given nutrient supply. To better understand the relationship between dynamically stable and unstable states we included the latter in our analysis. Fig. 3C shows the first vs the second principle components of relative microbial abundances sampled in this fluctuating environment. (two more examples calculated for different multistable neighborhoods are shown in Fig. S5A-B). One can see 5 distinct clusters each corresponding to a single dynamically stable uninvadable state. Interestingly, in the PCA plot these states are separated by $V - 1 = 4$ dynamically unstable ones. Furthermore, all states are aligned along a quasi-1D manifold with an alternating order of stable and unstable states.

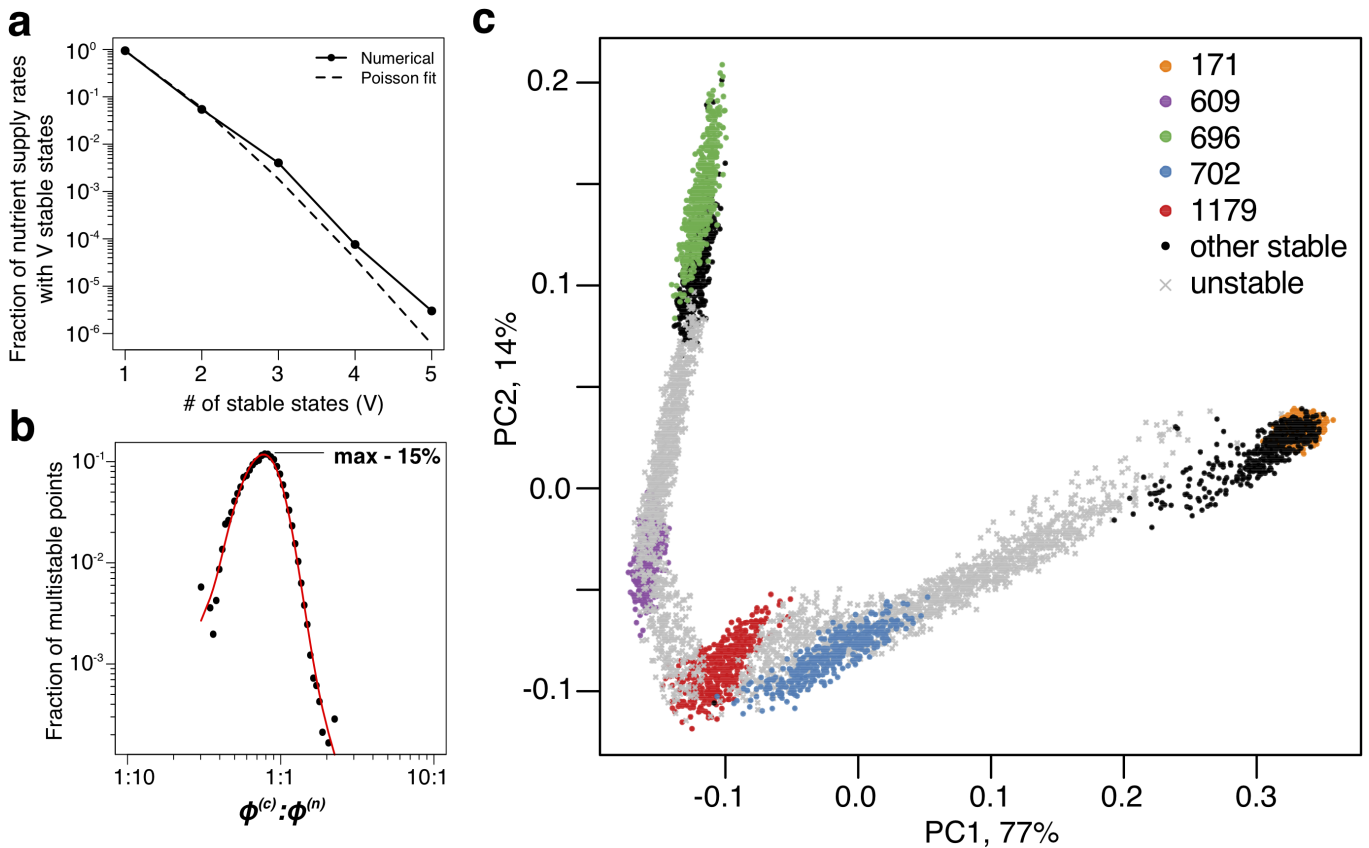


FIG. 3. **Patterns of multistability.** (a) The distribution of the number, V , of stable states across the entire space of nutrient supply rates. The data is based on Monte Carlo sampling of 1 million different environments (combinations of nutrient supply rates) in the $6C \times 6N \times 36S$ model. Solid circles show the fraction of all sampled environments for which $V = 1, 2, 3, 4, 5$ stable states are simultaneously feasible. The dashed line is the fit to the data with a Poisson distribution for $v - 1$ extra states giving rise to multistability. (b) Fraction of multistable cases for different ratios of supply of two essential nutrients. The peak of the distribution is close to the balanced supply ($\phi^{(c)} : \phi^{(n)} \simeq 1 : 1$). (c) The PCA plot of relative microbial abundances in the vicinity of the environment, where $V = 5$ stable states coexist. Supply rates were randomly sampled within $\pm 10\%$ from the initial environment. Each point shows the first (x-axis) and the second (y-axis) principal components of microbial abundances in every uninvadable state feasible for this combination of supply rates. Colored circles label the original five stable states, black circles - several other stable states, which became feasible for nearby supply rates, and grey crosses - dynamically unstable states feasible in this region of nutrient supply rates.

D. Patterns of diversity and stability

Above we demonstrated that multistable states are much more common for balanced nutrient supply rates, that is to say, when the average ratio of carbon and nitrogen supply rates matches the average C:N stoichiometry of species in the community (see Fig. 3B). Interestingly, a balanced supply of nutrients also promotes species diversity. In Fig. 4A we plot the average number of species in a stable state, referred to as species richness, as a function of the average balance between carbon and nitrogen supplies for $6C \times 6N \times 36S$ model. The species richness is the largest (around 10.5) for balanced nutrient supply rates, while dropping down to the absolute minimal value of 6 in two extreme cases of very large imbalance of supply rates, where the nutrient supplied in excess becomes irrelevant in competition. In this case only 6 species that

are top competitors for carbon metabolites (if nitrogen supply is plentiful) or, respectively nitrogen metabolites (if carbon is large) survive, while the rest of less competitive species are never present in uninvadable states.

For balanced nutrient supply rates the relationship between species' competitiveness and its prevalence in the community is much less pronounced. It is shown in Fig. 4B where we plot the prevalence of the species as a function of its average competitiveness. Here the *average competitiveness* of a species is defined as the mean of its rank to compete for its carbon and nitrogen resources. The rank 1 being assigned to the most competitive species for a given resource (species with the largest value of λ), while the rank 6 - to the least competitive species for this resource. Species *prevalence* is given by the fraction of all environments where it can survive. Note that all 36 species in our pool are present in some of the environments.

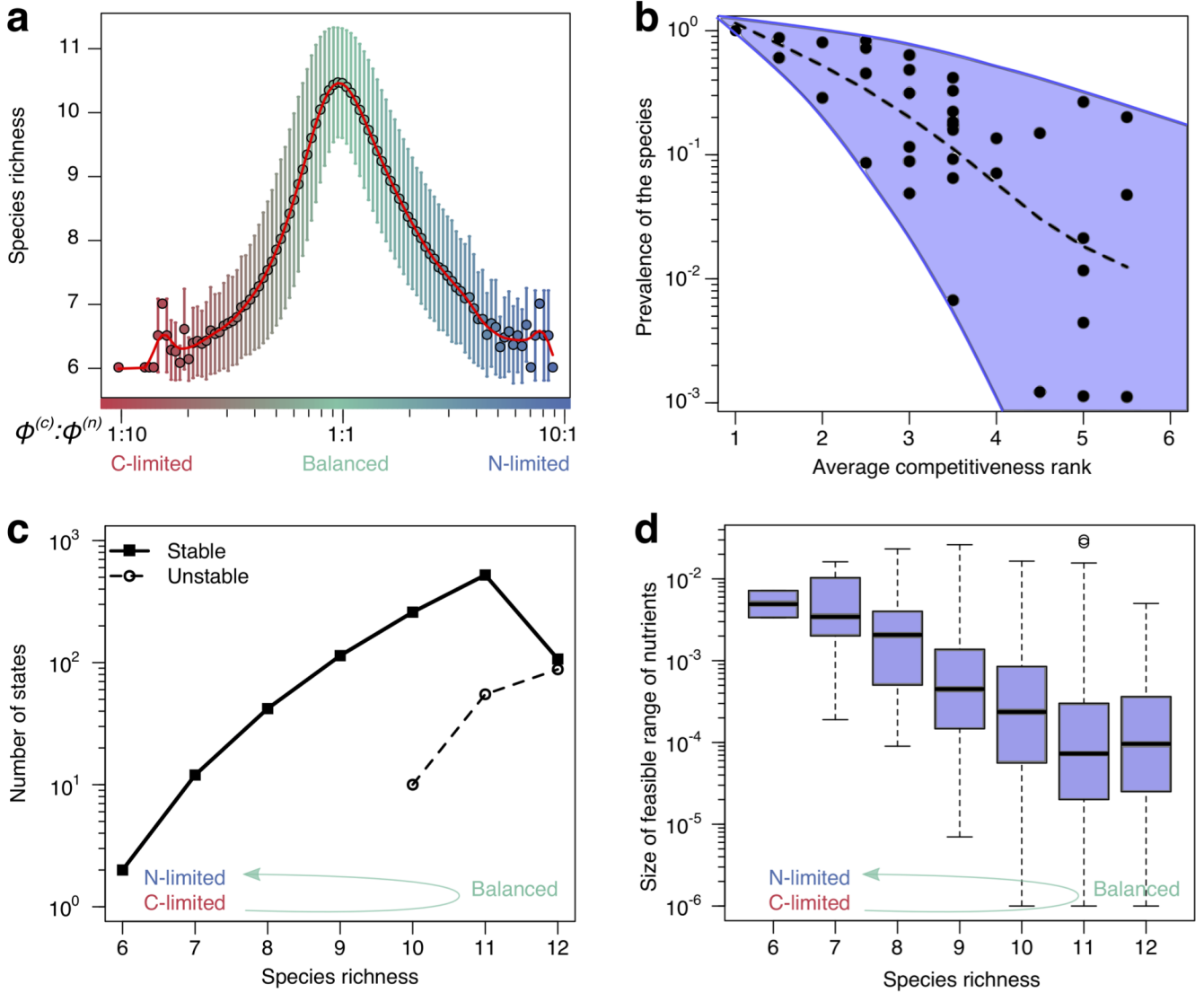


FIG. 4. **Patterns of diversity and stability** (a) Average species richness (y-axis) of uninvadable stable states feasible for a given $\phi^{(c)}:\phi^{(n)}$ nutrient supply ratio (x-axis). Error bars correspond to standard deviation of species richness of individual states feasible for a given nutrient supply ratio. (b): Scatter plot of the prevalence (y-axis) of each of the 36 species in the $6C \times 6N \times 36S$ model plotted vs its average competitiveness rank for its carbon and nitrogen sources. The latter is calculated from the rank order of $\lambda^{(c)}$ and $\lambda^{(n)}$ among all species consuming each resource (rank 1 corresponds to the largest λ for this resource among all species). Species prevalence is quantified as the fraction of environments where a given species can survive. The dashed line shows the average trend. (c) The number of uninvadable dynamically stable (solid line) and unstable (dashed line) states with a particular species richness (x-axis). (d) Boxplot of nutrient feasibility ranges of uninvadable stable states plotted as a function of their species richness. All plots were calculated for the $6C \times 6N \times 36S$ model.

In general more competitive species tend to survive in a larger subset of environments (see the dashed curve in Fig. 4B). For example, in our pool there is one species which happens to be the most competitive for both its carbon and nitrogen sources. This species is present in all of the states in every environment. However, we also find that some of the least competitive species (those at the right end of the x-axis in Fig. 4B) survive in a broad range of environments. For example, one species with average competitiveness rank of 5.5 corresponding

to the last and next to last rank for its two resources still has relatively high prevalence of around 20%. This illustrates complex ways in which relative competitiveness of all species in the pool shapes their prevalence in a broad range of environments.

We also explore the relationship between species richness of a state (i.e., its total number of surviving species) and its other properties. Fig. 4C shows an exponential increase of the number of uninvadable states as a function of species richness. In our $6C \times 6N \times 36S$ model all

uninvadable states with less than 10 species are dynamically stable (solid line in Fig. 4C), while those with 10 or more species can be both stable or unstable (dashed line in Fig. 4C). Overall the fraction of stable states to dynamically unstable ones decreases with species richness. In other words, the probability for a state to be dynamically unstable increases with the number of species. In this aspect our model behaves similar to the gLV model in Robert May's study³⁵.

In Fig. 4D we show a negative correlation between the species richness of a stable state and its feasible range of nutrient supplies. Thus in our model the number of species in an ecosystem has a detrimental effect on the structural stability of the community quantifying its robustness to fluctuating nutrient supply³³. The empirically observed exponential decay of state's feasible range with its number of species is well described by a two-fold decrease per each species added (see Ref.³⁷ and³⁴ for related results in the gLV model). Note that the observed decrease in feasible range with species richness goes hand-in-hand with an increase in the overall number of states. Thus in well-balanced environments a large number of states are carving all possible combinations of nutrient supply into many small and overlapping ranges.

Overall the results of our model with a large number of nutrients suggest the following picture. In nutrient-balanced environments we expect to observe a high diversity of species in the existing communities. These species can form a very large number of possible combinations (uninvadable states). Each of these states could be realized only for a narrow range of nutrient supply rates indicating their low structural stability. Moreover in such environments we predict common appearance of multistability between some of these states.

II. DISCUSSION

The inspiration for our model was the common appearance of alternative stable states in ecosystems in general, and microbial communities in particular^{5,6,10,13-16}. To the best of our knowledge our model is the first resource-explicit model capable of multistability between several states each characterized by a high diversity of species. We extend Tilman's scenario²⁸ in which the growth of two species is limited by a pair of essential resources to the case of multiple nutrients of each type. This allows us to assemble complex communities with large number of co-existing species and provides additional insights into patterns of multistability in such communities.

A. Multistability requires diverse species stoichiometry and balanced nutrient supply

We find that multistability of microbial communities in our model requires species with different nutrient stoichiometries – which is known to be highly variable in

real microbes³⁸. In this aspect our model is similar to both the Tilman model²⁸, and the MacArthur family of models^{17,18,39}. In common variants of the MacArthur model, the multistability is absent due to the assumption of identical nutrient yields of different species²⁰⁻²⁴. However, MacArthur model with different nutrient yields of different species should be capable of multistability. The larger is the variation of C:N stoichiometries of individual species in our model, the higher is the likelihood to observe multistability Fig. S4. Somewhat unexpectedly, at least in the $2C \times 2N \times 4S$ model about half of the combinations of stoichiometries yielded no multistable states at all. Hence, variable stoichiometries do not guarantee multistability unless they are combined with the right combination of species competitiveness (see Section in Supplementary Materials for mathematical arguments of why that may be the case).

Another important factor favoring multistability in our model is the balanced supply of two essential nutrients (see Fig. 3B). It occurs when the average ratio of supply rates of two essential nutrients matches the average C:N stoichiometry of community's species (see Fig. 3B). When nutrient supplies are balanced, microbial community multistability is relatively common. Furthermore, for balanced nutrients the community can be in one of many different states, characterized by different combinations of limiting nutrients. These states tend to have high species diversity (Fig. 4A) - a trend consistent with lake ecosystems in Ref.⁴⁰, and relatively small range of feasible supply rates (Fig. 4D). Hence, regime shifts can be easily triggered by changes in nutrient supply. The balanced region is characterized by a complex relationship between species competitiveness and survival, so that even relatively poor competitors could occasionally have high prevalence (species in the upper right corner of Fig. 4B).

In the opposite limit the supply of nutrients of one type (say nitrogen) greatly exceeds that of another type (say carbon). For such imbalanced supply the community has a unique uninvadable state, where every carbon nutrient supports the growth of the single most competitive species. Nitrogen nutrients are not limiting the growth of any species and thus have no impact on species survival and community diversity. As a consequence, the average diversity of microbial communities in such nutrient-imbalanced environments is low (about one half of that for balanced supply conditions). This is in agreement with many experimental studies showing that addition of high quantities of one essential nutrient (e.g. as nitrogen fertilizer) tends to decrease species diversity. This has been reported in numerous experimental studies cited in the chapter "Resource richness and species diversity" of Ref.²⁸ as well as in recent experiments in microbial communities⁴¹.

B. Interplay between diversity and stability in ecosystems with multiple essential nutrients

Ever since Robert May’s provocative question “Will a large complex system be stable?”³⁵ the focus of many theoretical ecology studies has been on investigating the interplay between dynamic stability and species diversity in real and model ecosystems⁴². May’s prediction that ecosystems with large number of species tend to be dynamically unstable needs to be reconciled with the fact that we are surrounded by complex and diverse ecosystems that are apparently stable. Thus it is important to understand the factors affecting stability of ecosystems in general and microbial ecosystems in particular .

Here we explored the interplay between diversity and stability in a particular type of microbial ecosystems with multiple essential nutrients. We discussed three criteria for stability of microbial communities shaped by the competition for nutrients: (i) how stable is the species composition of a community to fluctuations in nutrient supply rates; (ii) the extent of community’s resilience to species invasions; and (iii) its dynamical stability to small stochastic changes in abundances of existing species. Naturally-occurring microbial communities may or may not be stable according to either one of these three criteria⁴². The degree of importance of each single criterion is determined by multiple factors such as how constant are nutrient supply rates in time and space and frequently new microbial species migrate to the ecosystem.

Our model provides the following insights into how these three criteria are connected to each other. First, as evident from Fig. 1F, the three types of stability are largely independent from each other. Second, communities growing on a well balanced mix of nutrients tend to have high species diversity (see peak in Fig. 4A). However, each of the community states in this regime tends to have a low structural stability with respect to nutrient fluctuations. In environments with highly variable nutrient supplies the community will frequently shift between these states. That is to say, some of the species will repeatedly go locally extinct and the vacated niches will be repopulated by others. Furthermore, many of the steady states in this regime are dynamically unstable giving rise to multistability and regime shifts. In this sense our model follows the general trend reported in Ref.³⁵. Conversely, microbial communities growing on an imbalanced mix of essential nutrients have relatively low diversity (Fig. 4A) but are characterized by a high degree of structural and dynamic stability (see Fig. 4D and Fig. 4C respectively).

The existence of dynamically unstable states always goes hand in hand with multistability⁹ (see Fig. 2B for an illustration of this effect in our model). Interestingly, in our model we always find $V - 1$ dynamically unstable states coexisting with V dynamically stable ones for the same environmental parameters (see Fig. 3C and Fig. S5 for some examples). All states (both dynamically sta-

ble and unstable) shown in Fig. 3C are positioned along some one-dimensional curve in PCA coordinates. This arrangement hints at the possibility of a non-convex one-dimensional Lyapunov function whose V minima (corresponding to stable states) are always separated by $V - 1$ maxima (unstable stable states) as dictated by the Morse theory⁴³. This should be contrasted with convex multi-dimensional Lyapunov functions used in Refs.^{18,39,44}.

C. Extensions of the model

Our model can be extended to accommodate several additional properties of real-life microbial ecosystems: First, one could include generalist species capable of using more than one nutrient of each type. The growth rate of such species is given by:

$$g_{\alpha} = \min \left(\sum_{i \text{ used by } \alpha} \lambda_{\alpha i}^{(c)} c_i, \sum_{j \text{ used by } \alpha} \lambda_{\alpha j}^{(n)} n_j \right)$$

Here the sum over i (respectively j) is carried out over all carbon (respectively nitrogen) sources that this species is capable of converting to its biomass. One may also consider the possibility of diauxic shifts between substitutable nutrient sources. In this case each generalist species is following a predetermined preference list of nutrients and uses its carbon and nitrogen resources one-at-a-time, as modelled in Ref.²³. Since at any state each of the species is using a “specialist strategy”, that is to say, it is growing on a single carbon and a single nitrogen source, we expect that many of the results of this study would be extendable to this model variant. Interestingly, the stable marriage problem can be used to predict the stable states of microbial communities with diauxic shifts between substitutable resources²³ and those in communities growing on a mix of two essential nutrients as in this study. It must be pointed out that these models use rather different variants of the stable marriage model.

It is straightforward to generalize our model to Monod’s growth equation and to take into account non-zero death rate (or maintenance cost) of individual species (see Supplementary Materials section).

One can extend our model to include cross-feeding between the species. In this case some of the nutrients are generated as metabolic byproducts by the species in the community. These byproducts should be counted among nutrient sources and thus would allow the number of species to exceed the number of externally-supplied resources.

Above we assumed a fixed size of the species pool. This constraint could be modified in favor of an expanding pool composed of a constantly growing number of species. These new species correspond to either migrants from outside of or mutate from outside of the community or mutants of the species within the community. This variant of the model would allow one to explore the interplay between ecosystem’s maturity (quantified by the

number of species in the pool) and its properties such as multistability and propensity to regime shifts.

D. Control of microbial ecosystems exhibiting multistability and regime shifts

In many practical situations we would like to be able to control microbial communities in a predictable and robust manner. That is to say, we would like to be able to reliably steer the community into one of its stable states and to maintain it there for as long as necessary. Alternative stable states and regimes shifts greatly complicate the task of manipulation and control of microbial ecosystems. Indeed, multistability means that the environmental parameters alone do not fully define the state of the community. In order to get it to a desired state, one needs to carefully select the trajectory along which one changes the environmental parameters (nutrient supply rates). Changing these parameters could lead to disappearance (local extinction) of some microbial species and open the ecosystem for colonization by others thereby changing its state. Densely interconnected networks of regime shifts shown in Fig. 2E-F can be viewed as maps guiding the selection of the optimal trajectory to the desired stable species composition. The exploration of different manipulation strategies of microbial ecosystems is the subject of our future research⁴⁵.

III. ACKNOWLEDGMENTS

Part of this work has been carried out at the University of Padova, Italy, in August 2018, during a scientific visit by one of us (S.M.). The authors wish to thank Prof. James O'Dwyer, Prof. Seppe Kuehn and Akshit Goyal for a critical reading of an earlier version of the manuscript.

IV. AUTHORS CONTRIBUTIONS

S.M. designed the research; P.P. simulated the computational model; Y.F. and S.M. developed the theory and mapped this model to the stable marriage problem; P.P., S.M., and V.D. analyzed the data; S.M., V.D., and Y.F. wrote the manuscript; S.M. supervised the study.

V. METHODS

A. Identification of all states and classification of them as invadable or uninvadable

The competitive exclusion principle states that, in general, two species competing for the same growth-limiting nutrient cannot coexist with each other. Accounting for non-limiting nutrients present in our model, the competitive exclusion principle can be reformulated as the following two rules:

- Rule 1: In a given steady state each nutrient (either carbon or nitrogen) limits the growth of no more than one species.
- Rule 2: Any number of species can use a given nutrient in a non growth-limiting fashion. However, each of such species needs to be able to survive given the steady state concentration of this nutrient set by the growth-limited species. That means that for every nutrient each of the non growth-limited species β needs to be more competitive than the grow-limited species α for the same resource: $\lambda_{\alpha}^{(c)} < \lambda_{\beta}^{(c)}$ (or $\lambda_{\alpha}^{(n)} < \lambda_{\beta}^{(n)}$ in case of a nitrogen nutrient).

Note that in any state of our model every species has a unique nutrient limiting its growth. By the virtue of the Rule 1, if a nutrient is limiting the growth of any species at all, such species is also unique. Hence, in a given state the relationship between surviving species and their growth-limiting nutrients (marked as shaded ovals in Fig. 1A) is an example of a matching on a graph of resource utilization. Rule 2 imposes additional limitations on this matching. As we show in the Supplementary Material, section), uninvadable states correspond to stable matchings in a variant of the celebrated stable marriage problem^{29,30}.

Just like in the MacArthur model¹⁷ or any other resource-explicit model for that matter, the number of species present in a steady state of the community cannot exceed the total number of nutrients they consume. Any community constructed using Rules 1 and 2 represent a steady state of the ecosystem feasible for a certain range of nutrient supply rates. This state can be either invadable or uninvadable, and either dynamically stable or not.

For simplicity we work with an equal numbers of C and N resources (L carbons and L nitrogens), with one unique species capable of utilization of every pair of resources (L^2 species in total). We first selected the values of $\lambda_{(i,j)}^{(c)}$ and $\lambda_{(i,j)}^{(n)}$ from a uniform random distribution between 10 and 100. Note that all steady states of the community can be identified and tested for invadability using only the relative rank order of species' competitiveness for nutrients. For this we used the following exhaustive search algorithm:

Step 1 - Select the subset of species whose growth is limited by C (C-limited species). For every carbon nutrient there are L ways to choose a C-limited species using this nutrient. Based on Rule 1 such C-limited species will be unique. There is also an additional possibility that this nutrient is not limiting growth of any species. The total number of possibilities is $L + 1$ for each of L carbon nutrients. Thus, there are $(L + 1)^L$ ways to choose the set of C-limited species and our algorithm will exhaustively investigate each of these possibilities one-by-one.

Step 2 - Given the set of C-limited species selected in Step 1, we now select all N-limited species. We first eliminate from our search any species that doesn't have enough carbon to grow. That is to say, we go over all carbon nutrients one-by-one and eliminate all species whose $\lambda^{(c)}$ is smaller than that of the C-limited species (if any) for this carbon nutrient. Among the remaining species we go over the nitrogen nutrients one-by-one and look for all possible ways to add a species limited by a given nitrogen source n_j and satisfy the Rule 2. More specifically, we identify all species that use n_j and can grow on their carbon sources (those species remained after the elimination procedure described above). We then compare $\lambda^{(n)}$ s of these species to $\lambda^{(n)}$ s of all C-limited species using n_j . To satisfy the Rule 2 for each n_j we can add at most one N-limited species and its $\lambda^{(n)}$ has to be smaller than $\lambda^{(n)}$ s of all C-limited species using n_j . Let M_j be the number of such species ($M_j = 0$ if there are no such species for a given n_j). The total number of possible steady states of our model for a given combination of C-limited species selected in Step 1 is given by $\prod_{j=1}^L (M_j + 1)$. Here the factor $M_j + 1$ takes into account an additional possibility to have no N-limited species for n_j .

The unique way to construct an uninvadable state by following this algorithm is to go over all nitrogen sources one-by-one and for each of them attempt to add the N-limited species with the largest $\lambda^{(n)}$ among all species using this resource, whose growth is allowed by carbon constraints. If for every n_j this species is allowed by the Rule 2, that is to say, if its $\lambda^{(n)}$ is smaller than $\lambda^{(n)}$ of all C-limited species using n_j , we successfully constructed a unique uninvadable state for a given set of C-limited species. Indeed, all possible invading species that are allowed to grow by their carbon nutrients will be blocked by their nitrogen nutrients. If, however, for any of n_j , the species with the largest $\lambda^{(n)}$ is not allowed by the Rule 2, that is to say, if its $\lambda^{(n)}$ is larger than $\lambda^{(n)}$ of at least one of the C-limited species, this species would make a successful invader of any state we construct. In this case there is no uninvadable state for the set of C-limited species selected during the Step 1.

We used the above procedure to identify all possible steady states and to classify them as invadable and uninvadable for different numbers of resources used in our $2C \times 2N \times 4S$ and $6C \times 6N \times 36S$ examples. Note that, while this method is computationally possible for relatively small number of nutrients (we were able to successfully use it for up to 9 nutrients of each type), for larger

systems one should rely on computationally more efficient algorithms based on the stable marriage problem^{29,30} as described in the Supplementary Material section .

B. Monte-Carlo sampling of nutrient supply rates to identify feasible ranges of states

Given the parameters defining all species (i.e., the set of their λ s and Y s) and the chemostat dilution constant δ , each state p is feasible within a finite region in the nutrient supply space (a $K + M$ dimensional space $\vec{\Phi} = \{\phi_i^{(c)}, \phi_j^{(n)}\}$) where all microbial populations and nutrient concentrations are non-negative and the limiting nutrients of every surviving species do not change. It is easy to show that in a steady state our system satisfies mass conservation laws for each of the nutrients:

$$\begin{aligned} c_i + \sum_{\text{all } \alpha \text{ using } c_i} \frac{B_\alpha}{Y_\alpha^{(c)}} &= \frac{\phi_i^{(c)}}{\delta} \quad , \\ n_j + \sum_{\text{all } \alpha \text{ using } n_j} \frac{B_\alpha}{Y_\alpha^{(n)}} &= \frac{\phi_j^{(n)}}{\delta} \quad . \end{aligned} \quad (4)$$

To simplify the process of calculating the feasible volumes of all states we worked in the *limit of high nutrient supply* where $\phi_i^{(c)} \gg \frac{\delta^2}{\lambda_\alpha^{(c)}}$ and $\phi_j^{(n)} \gg \frac{\delta^2}{\lambda_\alpha^{(n)}}$ for all species α . In this case the concentration $\delta/\lambda_\alpha^{(c,n)}$ of any nutrient limiting growth of some species (α in this case) is negligible compared to its ‘‘abiotic concentration’’ $\phi_i^{(c,n)}/\delta$, that is to say, its concentration before any microbial species were added to the chemostat. In this case one can ignore the terms c_i and n_j in Eqs. 4 for all nutrient limiting growth of some species and leave only the ones that are not limiting the growth of any species. It is convenient to introduce the $K + M$ -dimensional vector \vec{X}_p of microbial abundances and non-limiting nutrient concentrations in a given state p . For example, for the uninvadable state #5 in the $2C \times 2N \times 4S$ model we have: $\vec{X}_5 = \{B_{(1,1)}, B_{(1,2)}, B_{(2,2)}, n_2\}$.

The mass conservation laws (Eq. 4) can be used to obtain the feasible volumes of all states and can be represented in a compact matrix form for each state p :

$$\vec{\Phi} = \hat{R}_p \vec{X}_p \quad , \quad (5)$$

where Φ is the vector of $K + M$ nutrient supply rates and \hat{R}_p is a matrix composed of inverse yields Y^{-1} of surviving species and ‘‘1’’ for each of the non-limiting nutrients in a given state p . For example, for the state #5 in our $2C \times 2N \times 4S$ model the Eq. 5 expands to:

D. Dynamic stability of states

$$\begin{bmatrix} \phi_1^{(c)} \\ \phi_2^{(c)} \\ \phi_1^{(n)} \\ \phi_2^{(n)} \end{bmatrix} = \begin{bmatrix} \frac{1}{Y_{(1,1)}^{(c)}} & \frac{1}{Y_{(1,2)}^{(c)}} & 0 & 0 \\ 0 & 0 & \frac{1}{Y_{(2,2)}^{(c)}} & 0 \\ \frac{1}{Y_{(1,1)}^{(n)}} & 0 & 0 & 0 \\ 0 & \frac{1}{Y_{(1,2)}^{(n)}} & \frac{1}{Y_{(2,2)}^{(n)}} & 1 \end{bmatrix} \begin{bmatrix} B_{(1,1)} \\ B_{(1,2)} \\ B_{(2,2)} \\ n_2 \end{bmatrix}. \quad (6)$$

Using Eq. 5 it is easy to check if a given state is feasible at a particular nutrient supply rate $\vec{\Phi}$ by multiplying \hat{R}_p^{-1} (the inverse of the matrix \hat{R}_p) with $\vec{\Phi}$. If all of the elements of the resulting vector \vec{X}_p are positive, then the state p is feasible at $\vec{\Phi}$. If the matrix \hat{R}_p is not invertible i.e., $\det(\hat{R}_p) = 0$, the state is feasible only on a low-dimensional subset of nutrient supply rates. This is not possible for a general choice of yields Y and is not considered in our study.

We imposed a common upper and lower bound on each of the $K + M$ nutrient supply rates ($\phi_{min} \leq \phi_i^{(c,n)} \leq \phi_{max}$) thus restricting the search of volumes of feasible states to a $(K + M)$ -dimensional hypercube in the nutrient supply space. We chose $\phi_{min} = 10, \phi_{max} = 1000$. The lower bound ensures that the system is always in the limit of high nutrient supply since $\max(\frac{\delta^2}{\lambda\alpha}) = 0.1 \ll \phi_{min} = 10$. We then randomly selected 10^6 nutrient supply rate combinations $\vec{\Phi}$ within these bounds (Monte Carlo sampling) and checked the feasibility of each of the 33 possible states in the $2C \times 2N \times 4S$ model and each of the 1211 uninvadable states in the $6C \times 6N \times 36S$ model. That is to say, for every set of nutrient supply rates $\vec{\Phi}$ and for every state p we checked whether all elements of \vec{X}_p are positive. The feasible range of nutrient supply rates of each state was estimated as the fraction of nutrient supply rate combinations (out of 1 million vectors $\vec{\Phi}$ sampled by our Monte Carlo algorithm) where it is feasible.

C. The network of regime shifts from overlaps of feasible ranges

Two stable states are said to be capable of a regime shift if their feasibility ranges overlap with each other, i.e. if there exists at least one nutrient supply rate combination at which both these states are feasible. We used the data obtained by the Monte-Carlo sampling to look for such cases and to construct networks shown in Fig. 2E, Fig. 2F. We used Gephi 0.9.2 software package to visualize the network in Fig. 2F and to perform its modularity analysis. Seven densely interconnected clusters shown with different colors in Fig. 2F were identified using Gephi's built-in module-detection algorithm⁴⁶ with the resolution parameter set to 1.5.

Each of the states in our model is either dynamically stable or dynamically unstable at all nutrient supply rates where it is feasible. We checked the dynamic stability of every 33 possible states (for the $2C \times 2N \times 4S$ model) and each of 1211 uninvadable states (for the $6C \times 6N \times 36S$ model) using the following two algorithms:

1. **Small perturbation analysis** For $2C \times 2N \times 4S$ example we prepared each allowed state at multiple nutrient supply rate combinations where this state is feasible and subjected it to small perturbations of steady state values of all nutrient concentrations and of all populations of species present in the state. We choose to perturb only the populations of species present in the state because an invadable state, by definition, would always be dynamically unstable against addition of a very small population of at least one invading species from the species pool. This instability should not render it dynamically unstable. The numerical integration of the system dynamics following a perturbation was done in C programming language using the CVODE solver library of the SUNDIALS package⁴⁷.
2. **Inference of state's dynamic stability from the pattern of its overlaps with other states** The number of uninvadable states (1211) in our $6C \times 6N \times 36S$ model was too large to be tested directly as we did for the $2C \times 2N \times 4S$ model. Their dynamic stability was instead inferred from our Monte-Carlo simulations listing all feasible uninvadable states for every sampled nutrient supply rate combination. We first identified 1022 uninvadable states which were the only feasible uninvadable state for at least one nutrient supply point. All such states should be dynamically stable, since for every nutrient supply rate there should be at least one uninvadable dynamically stable state representing the end point of system's dynamics. The remaining 173 uninvadable states which were feasible for at least one of 1 million sampled nutrient supply rates were labelled as potentially dynamically unstable. Note that in our Monte-Carlo analysis we only sampled a finite (albeit large) number of supply rate combinations. Thus it is entirely possible that we missed some crucial supply rate combinations for which one of these states was the only uninvadable state. Any such point would have rendered this state as dynamically stable. Such false assignments might lead to a violation of the basic empirical rule in our model stating that V uninvadable stable states are always accompanied by $V - 1$ uninvadable dynamically unstable states ($V/(V - 1)$ rule) for some sampled nutrient supply rates. In our Monte Carlo simulations of the $6C \times 6N \times 36S$ model the $V/(V - 1)$ rule was violated for only 370 nutrient

supply rates combinations out of 1,000,000 sampled points. We believe that these violations were caused by an incorrect identification of dynamically unstable states mentioned above. To iteratively refine the lists of stable and unstable states, we went over all potentially unstable states one-by-one and checked whether reclassifying the state involved in the largest number of violations as stable would reduce the overall number of violations. If it did, we reclassified this state as stable and recalculated the number of violations for all remaining points. By the end of this iterative procedure we were able to completely eliminate violations by reassigning 36 potentially unstable states as dynamically stable. This left us with $1022 + 36 = 1058$ dynamically stable and $173 - 36 = 137$ dynamically unstable uninvadable states in the $6C \times 6N \times 36S$ model. The remaining $1211 - 1058 - 137 = 16$ uninvadable states were not feasible for any of 1,000,000 sampled nutrient supply rates. Hence their dynamic stability remains unidentified. Both 36 reassigned states and 16 undetected states are expected to have very small ranges of feasible nutrient supply rates.

E. Multistability as a function of variation in stoichiometric ratios of different species

To investigate how the extent of multistability in our model depends on variation in stoichiometric ratios of different species, we simulated 4000 variants of the $2C \times 2N \times 4S$ model. In these variants we kept the same choice of species competitiveness (quantified

by their λ_s) but reassigned their yields Y . To cover a broad range of standard deviations of N:C stoichiometry of different species (their $Y_\alpha^{(c)}/Y_\alpha^{(n)}$) we randomly sampled yield combinations from gradually expanding intervals. First we simulated 1000 model variants, where yields of four species were independently drawn from $U(0.45, 0.55)$. These simulations were followed by 1000 model variants where yields of four species were drawn from $U(0.3, 0.7)$, 1000 model variants with yields from $U(0.1, 0.9)$ and, finally, 1000 model variants with yields from $U(0.01, 1.0)$. In each variant of the model with a particular set of yields of 4 species we calculated the fraction of multistable points among 10^5 nutrient supply rate combinations as described in the section of Methods.

The results are shown in Fig. S4. Its x-axis is the binned empirical standard deviation of species N:C stoichiometry equal to $Y^{(c)}/Y^{(n)}$, y-axis is the binned fraction of multistable nutrient supply rates, the color is proportional to \log_{10} of the fraction of yield combinations (out of 4000 sampled yield combinations) that belong to a given bin of x- and y-axes.

F. GitHub repository of the code used in our project

The PCA analysis, plots and statistical tests were implemented using R version 3.4.4. Other simulations were carried out in C (using compiler gcc version 5.4.0) and Python 3.5.2. Matlab analysis was done using MATLAB and Statistics Toolbox Release 2018a, The MathWorks, Inc., Natick, Massachusetts, United States. The code for both our simulations and statistical analysis can be downloaded from: <https://github.com/ssm57/CandN>.

* These three authors contributed equally

† maslov@illinois.edu

- ¹ X. Zhou, C. J. Brown, Z. Abdo, C. C. Davis, M. A. Hansmann, P. Joyce, J. A. Foster, and L. J. Forney, *The ISME journal* **1**, 121 (2007).
- ² L. Lahti, J. Salojrvi, A. Salonen, M. Scheffer, and W. M. d. Vos, *Nature Communications* **5**, ncomms5344 (2014).
- ³ C. A. Lozupone, J. I. Stombaugh, J. I. Gordon, J. K. Jansson, and R. Knight, *Nature* **489**, 220 (2012).
- ⁴ J. Zhou, W. Liu, Y. Deng, Y.-H. Jiang, K. Xue, Z. He, J. D. V. Nostrand, L. Wu, Y. Yang, and A. Wang, *mBio* **4**, e00584 (2013).
- ⁵ E. Pagaling, K. Vassileva, C. G. Mills, T. Bush, R. A. Blythe, J. Schwarz-Linek, F. Strathdee, R. J. Allen, and A. Free, *Environmental microbiology* **19**, 3374 (2017).
- ⁶ D. Gonze, L. Lahti, J. Raes, and K. Faust, *The ISME journal* **11**, 2159 (2017).
- ⁷ A. Shade, H. Peter, S. D. Allison, D. Baho, M. Berga, H. Bürgmann, D. H. Huber, S. Langenheder, J. T. Lennon, J. B. Martiny, *et al.*, *Front. Microbiol.* **3**, 417 (2012).
- ⁸ J. C. Rocha, G. Peterson, Ö. Bodin, and S. Levin, *Science* **362**, 1379 (2018).

- ⁹ M. Scheffer and S. R. Carpenter, *Trends in ecology & evolution* **18**, 648 (2003).
- ¹⁰ J. P. Sutherland, *Amer Nat* **108**, 859 (1974).
- ¹¹ C. S. Holling, *Annu Rev Ecol Syst* **4**, 1 (1973).
- ¹² R. M. May, *Nature* **269**, 471 (1977).
- ¹³ D. Tilman, C. L. Lehman, and K. T. Thomson, *Proc. Natl. Acad. Sci. U.S.A.* **94**, 1857 (1997).
- ¹⁴ A. Schröder, L. Persson, and A. M. De Roos, *Oikos* **110**, 3 (2005).
- ¹⁵ T. Fukami and M. Nakajima, *Ecol Lett* **14**, 973 (2011).
- ¹⁶ T. Bush, M. Diao, R. J. Allen, R. Sinnige, G. Muyzer, and J. Huisman, *Nature Communications* **8**, 789 (2017).
- ¹⁷ R. MacArthur and R. Levins, *Proc. Natl. Acad. Sci. U.S.A.* **51**, 1207 (1964).
- ¹⁸ R. MacArthur, *Theoretical population biology* **1**, 1 (1970).
- ¹⁹ J. Huisman and F. J. Weissing, *Ecology* **82**, 2682 (2001).
- ²⁰ M. Tikhonov and R. Monasson, *Physical Review Letters* **118**, 048103 (2017).
- ²¹ A. Posfai, T. Taillefumier, and N. S. Wingreen, *Physical review letters* **118**, 028103 (2017).
- ²² J. E. Goldford, N. Lu, D. Bajić, S. Estrela, M. Tikhonov, A. Sanchez-Gorostiaga, D. Segrè, P. Mehta, and

- A. Sanchez, *Science* **361**, 469 (2018).
- ²³ A. Goyal, V. Dubinkina, and S. Maslov, *The ISME journal*, <https://doi.org/10.1038/s41396> (2018).
- ²⁴ S. Butler and J. O’Dwyer, *bioRxiv*, 293605 (2018).
- ²⁵ N. Fanin, S. Hättenschwiler, P. F. Chavez Soria, and N. Fromin, *Frontiers in microbiology* **6**, 1507 (2016).
- ²⁶ T. J. Browning, E. P. Achterberg, I. Rapp, A. Engel, E. M. Bertrand, A. Tagliabue, and C. M. Moore, *Nature* **551**, nature24063 (2017).
- ²⁷ T. Camenzind, S. Hättenschwiler, K. K. Treseder, A. Lehmann, and M. C. Rillig, *Ecological Monographs* **88**, 4 (2018).
- ²⁸ D. Tilman, *Monographs in population biology* **17**, 1 (1982).
- ²⁹ D. Gale and L. S. Shapley, *The American Mathematical Monthly* **69**, 9 (1962).
- ³⁰ D. Gusfield and R. W. Irving, *The stable marriage problem: structure and algorithms* (MIT press, 1989).
- ³¹ H. De Baar, *Progress in Oceanography* **33**, 347 (1994).
- ³² G. F. Gause, *Journal of experimental biology* **9**, 389 (1932).
- ³³ R. P. Rohr, S. Saavedra, and J. Bascompte, *Science* **345**, 1253497 (2014).
- ³⁴ J. Grilli, M. Adorisio, S. Suweis, G. Barabás, J. R. Banavar, S. Allesina, and A. Maritan, *Nature communications* **8**, 14389 (2017).
- ³⁵ R. M. May, *Nature* **238**, 413 (1972).
- ³⁶ S. Allesina and S. Tang, *Nature* **483**, 205 (2012).
- ³⁷ C. A. Servn, J. A. Capitn, J. Grilli, K. E. Morrison, and S. Allesina, *Nature Ecology and Evolution* **2**, 1237 (2018).
- ³⁸ K. Vrede, M. Heldal, S. Norland, and G. Bratbak, *Appl. Environ. Microbiol.* **68**, 2965 (2002).
- ³⁹ P. Chesson, *Theoretical Population Biology* **37**, 26 (1990).
- ⁴⁰ S. J. Interlandi and S. S. Kilham, *Ecology* **82**, 1270 (2001).
- ⁴¹ B. L. Mello, A. M. Alessi, S. McQueen-Mason, N. C. Bruce, and I. Polikarpov, *Scientific reports* **6**, 38781 (2016).
- ⁴² A. R. Ives and S. R. Carpenter, *science* **317**, 58 (2007).
- ⁴³ J. Milnor, *Morse Theory*, Vol. 51 (Princeton university press, 1963).
- ⁴⁴ T. J. Case and R. G. Casten, *Amer Nat* **113**, 705 (1979).
- ⁴⁵ S. Maslov, A. Goyal, V. Dubinkina, P. P. Pandey, and Y. Fridman, manuscript in preparation (2019).
- ⁴⁶ V. D. Blondel, J.-L. Guillaume, R. Lambiotte, and E. Lefebvre, *Journal of statistical mechanics: theory and experiment* **2008**, P10008 (2008).
- ⁴⁷ A. C. Hindmarsh, P. N. Brown, K. E. Grant, S. L. Lee, R. Serban, D. E. Shumaker, and C. S. Woodward, *ACM Transactions on Mathematical Software (TOMS)* **31**, 363 (2005).
- ⁴⁸ K. Kovarova-Kovar and T. Egli, *Microbiology and molecular biology reviews* : MMBR **62**, 646 (1998).
- ⁴⁹ F. G. Bader, *Biotechnology and Bioengineering* **20**, 183 (1978).
- ⁵⁰ A. V. Tkachenko and S. Maslov, *bioRxiv*, 204826 (2017).
- ⁵¹ S. Maslov, unpublished (2018).

VI. SUPPLEMENTARY MATERIAL

A. General form of growth laws

It is straightforward to generalize our model to allow a more general functional form for growth laws than Liebig’s law, $\min(\lambda_\alpha^{(c)} c_i, \lambda_\alpha^{(n)} n_j)$. Microbial growth on two essential substrates is thought to normally follow Monod’s equation for the rate-limiting nutrient: $g_\alpha^{(m)} \min(c_i/(K_\alpha^{(c)} + c_i), n_j/(K_\alpha^{(n)} + n_j))$ (See Ref.⁴⁸ for a discussion of limitations of Monod’s law). For low concentrations of the rate-limiting nutrient, say carbon source, the Monod’s law simplifies to the linear growth law used throughout this study: $g_\alpha = \lambda_\alpha^{(c)} c_i$. Microbes’ competitive abilities, also known as their specific affinities towards each substrate, are related to the parameters of Monod’s law via

$$\lambda_\alpha^{(c)} = \frac{g_\alpha^{(m)}}{K_\alpha^{(c)}}; \quad \lambda_\alpha^{(n)} = \frac{g_\alpha^{(m)}}{K_\alpha^{(n)}} \quad (S1)$$

In another variant of growth laws, two essential nutrients at low concentrations jointly affect the growth rate of the microbe: $g_\alpha^{(m)} c_i \cdot n_j / [(K_\alpha^{(c)} + c_i) \cdot (K_\alpha^{(n)} + n_j)]$ (see Ref.⁴⁹ for a discussion of these and other forms of double-substrate growth law). For simplicity of mathematical calculation we limited this study to Liebig’s law. However, many of the essential results we obtained (e. g. possible multistability in a system where species have different yields) hold for any growth laws listed above. In fact, the low concentration version of the previous growth law, where $g_\alpha^{(m)} c_i \cdot n_j$ has been studied by one of us in the context of autocatalytic growth of heteropolymers⁵⁰. Instead of exponentially replicating microbial species Ref.⁵⁰ considers pairs of mutually catalytic (and thus exponentially growing) complementary “2-mers” (a specific sequence of two consecutive monomers anywhere within a polymer chain). This minor difference complicates the math, while leaving the basic properties unchanged. Just like in our system, where up to $2L$ species (out of L^2 candidates) may simultaneously survive in the steady state of an ecosystem grown on of L carbon and L nitrogen sources, the polymer systems have no more than $2Z$ 2-mer “species” (out of Z^2 candidates) surviving in the steady state with polymers having Z possible monomers on their right ends and Z possible monomers on their left ends. Many (but not all) results of this paper are largely consistent with the present study. Note that for polymers the yields of all “species” are equal to 1, that is to say, one new 2-mer is formed upon ligation of one left end of a polymer with one right of another polymer chain. Yet, the model in Ref.⁵⁰ is capable of (at least) bistability. At present, it is not clear if this is due to autocatalytic cycles having length 2 or this property would survive in a simpler version of the model in which instead of the Eq. (1) of Ref.⁵⁰ one has

$$\dot{d}_{ij} = d_{ij}(\lambda_{ij}l_i r_j - \delta)$$

and the overall fluxes of left and right ends are independent from each other (instead of both being equal to $c_i = \phi_i/\delta$ as in Ref.⁵⁰).

Another variant of the model is where each species α has its own unique “death” or “maintenance” rate δ_α , playing the role of the same dilution rate δ . The steady states of this model (but not the dynamics leading to these states) can be calculated by dividing both sides of equations 2 by δ_α . This is equivalent by redefining the competitiveness parameters to $\tilde{\lambda}_\alpha = \lambda_\alpha/\delta_\alpha$ and setting the chemostat dilution rate to $\tilde{\delta} = 1$. All of our results in the high-flux regime $\phi \gg \delta^2/\lambda$ would remain unchanged.

From (Eq. 5-Eq. 6) one can see that when all species have the same C:N stoichiometry, the maximal number of microbial species in a state is equal to the number of nutrients minus 1. Indeed, one can show that a state p with $S_{surv} = K + M$ has $\det(\hat{R}_p) = 0$, which means that the feasible volume of any such state is zero. These states are only possible on a lower-dimensional manifold in the $(K + M)$ -dimensional space of supply rates (these results have been already discussed by Tilman in his special case²⁸).

Multistability is also possible in a variant of the MacArthur model^{17,18,39} in which different species have different yields on individual carbon sources⁵¹. A convex Lyapunov function¹⁸ precluding multistability does not exist in this case.

B. Constraints on steady states from microbial and nutrient dynamics

A steady state of equations describing the microbial dynamics (Eq. 2) is realized when either $B_\alpha = 0$ (the species was absent from the system from the start or subsequently went extinct) or when its growth rate g_α is exactly equal to the chemostat dilution rate δ . This imposes constraints on steady state nutrient concentrations with the number of constraints equal to the number of microbial species present with non-zero concentrations. Since, in general, the number of constraints cannot be larger than the number of constrained variables, no more than $K + M$ of species could be simultaneously present in a steady state of the ecosystem. For Liebig’s growth law used in this study, each resource can have no more than one species for which this resource limits its growth, that is to say, which sets the value of the minimum in $\min(\lambda_\alpha^{(c)} c_i, \lambda_\alpha^{(n)} n_j)$. The steady state concentrations of these resources are given by $c_i^{(*)} = \delta/\lambda_\alpha^{(c)}$ (if the growth is limited by the carbon source) and $n_j^{(*)} = \delta/\lambda_\alpha^{(n)}$ (if the growth is limited by the nitrogen source). Here α is the species whose growth is rate-limited by the resource in question. In a general case, no more than one species

can be limited by the same resource (carbon in our example), since the species with the largest $\lambda^{(c)}$ would out-compete other species with smaller values of $\lambda^{(c)}$ by making the steady state concentration $c_i^{(*)}$ so low that other species can no longer grow on it. Note however, that multiple species β could consume the same resource as the rate-limiting species α , as long as their growth is not limited by the resource. Each of these species must then be limited by their other nutrient (a nitrogen source in our example). However, their survival requires that carbon concentration set by species α is sufficient for their growth. Thereby, any species growing on a resource in a non-limited fashion must have $\lambda_\beta^{(c)} > \lambda_\alpha^{(c)}$.

Mathematically, it can be proven by observing that, since species β is limited by its nitrogen resource, one must have $\lambda_\beta^{(c)} c_i^{(*)} > \lambda_\beta^{(n)} n_j^{(*)}$. At the same time in a steady state, the concentrations of all rate-limiting resources are determined by the dilution rate δ via $\lambda_\beta^{(n)} n_j^{(*)} = \delta$, and $\lambda_\alpha^{(c)} c_i^{(*)} = \delta$. Combining the above three expressions one gets: $\lambda_\beta^{(c)} c_i^{(*)} > \lambda_\beta^{(n)} n_j^{(*)} = \delta = \lambda_\alpha^{(c)} c_i^{(*)}$, or simply $\lambda_\beta^{(c)} > \lambda_\alpha^{(c)}$. The constraints on competitive abilities λ for species present in a steady state in our model are then:

- Exclusion Rule 1: Each nutrient (either carbon or nitrogen source) can limit the growth of no more than one species α . From this it follows that the number of species co-existing in any given steady state cannot be larger than $K + M$, the total number of nutrients.
- Exclusion Rule 2: Each nutrient (e.g. specific carbon source) can be used by any number of species in a non-rate-limiting fashion (that is to say, where it does not constrain species growth in Liebig’s law). However, any such species β has to have $\lambda_\beta^{(c)} > \lambda_\alpha^{(c)}$, where $\lambda_\alpha^{(c)}$ is the competitive ability of the species whose growth is limited by this nutrient. In case of a nitrogen nutrient, the constraint becomes $\lambda_\beta^{(n)} > \lambda_\alpha^{(n)}$.

Note that the steady state solutions of equations Eq. 2 do not depend on populations B_α of surviving species. Their steady state populations $B_\alpha^{(*)}$ are instead determined by Eq. 3. Taking into account that, in a steady state, the growth rate of each surviving species is exactly equal to the dilution rate δ of the chemostat, after simplifications one gets:

$$\begin{aligned} \frac{\phi_j^{(c)}}{\delta} &= c_i^{(*)} + \sum_{\text{all } \alpha \text{ using } c_i} \frac{B_\alpha^{(*)}}{Y_\alpha^{(c)}} \\ \frac{\phi_j^{(n)}}{\delta} &= n_j^{(*)} + \sum_{\text{all } \alpha \text{ using } n_j} \frac{B_\alpha^{(*)}}{Y_\alpha^{(n)}} \end{aligned} \quad (\text{S2})$$

As described above, the steady state concentration of resources are given by $\delta/\lambda_\alpha^{(c \text{ or } n)}$, where α are the species

rate-limited by each resource. In the absence of such species, the concentration of a resource is given by anything left after it being consumed by surviving species in a non-rate-limiting manner. One can show that in this case, the resource (e.g. carbon) concentration has to be larger than $\delta/\lambda_\beta^{(c)}$, where $\lambda_\beta^{(c)}$ is the smallest affinity among microbes utilizing this resource.

One convenient approximation greatly simplifying working with Eq. S2 is the “high-flux limit” in which $\phi_i^{(c)} \gg \delta^2/\lambda_\alpha^{(c)}$ and $\phi_j^{(n)} \gg \delta^2/\lambda_\alpha^{(n)}$. In this approximation one can approximately set to zero the steady state concentrations of all resources that have a species rate-limited by them. The steady state concentrations of the remaining resources can take any value as long as it is positive. Hence, in this limit the Eq. S2 can be viewed as a simple matrix test of whether a given set of surviving species limited by a given set of resources is possible for a given set of nutrient fluxes. Indeed, multiplying the vector of fluxes with the inverse of the matrix \tilde{R} composed of inverse yields of surviving species and 1 for nutrients not limiting the growth of any species one formally gets the only possible set of steady state species abundances, $B_\alpha^{(*)}$, and a subset of non-limiting resource concentrations $c_i^{(*)}$ and $n_j^{(*)}$. If all of them are strictly positive - the steady state is possible. If just one of them enters the negative territory - the steady state cannot be realized for these fluxes of nutrients.

The above rule can be modified to apply even below the high-flux limit with the following modifications: 1) Instead of $\phi^{(c)}$ (or $\phi^{(n)}$), one uses their “effective values” $\tilde{\phi}^{(c)}$ (or $\tilde{\phi}^{(n)}$) introduced in²³, determined as

$$\begin{aligned} \tilde{\phi}_i^{(c)} &= \phi_i^{(c)} - \frac{\delta^2}{\lambda_{\alpha(i)}^{(c)}} \\ \tilde{\phi}_j^{(n)} &= \phi_j^{(n)} - \frac{\delta^2}{\lambda_{\alpha(j)}^{(n)}} \end{aligned} \quad , \quad (\text{S3})$$

where $\alpha(i)$ is the (unique) species limited by the nutrient i . If the nutrient is not limiting for any of the species in the steady state, $\alpha(i)$ is the species using the nutrient in a non-limited fashion, which has the *smallest* value of λ . This last rule comes from the observation that in order for a non-limiting resource not to become limiting for a species β currently using it in a non-limiting fashion, its concentration cannot fall below $\delta/\lambda_\beta^{(x)}$. Thus, when checking the feasibility of a given state, the concentration of a non-limiting resource can be written as $\delta/\lambda_\beta^{(x)} + a$ positive number, or (more conveniently) the influx of this resource can be offset as described in Eqs. S3

C. Stable matching approach for identification and classification of steady states

First we describe the exact one-to-one mapping between all uninvadable steady states (UIS) in our model

and the complete set of “stable marriages” in a variant of a well-known stable marriage or stable allocation problem developed by Gale and Shapley in the 1960s²⁹ and awarded the Nobel prize in economics in 2012. This mapping provides us with constructive algorithms to identify and count all uninvadable steady states in our ecosystem.

We start by considering a special case of our problem with L carbon and L nitrogen sources and a pool of L^2 species, such that for every pair of sources c_i (carbon) and n_j (nitrogen) there is exactly one microbe B_{ij} capable of using them. For the sake of simplicity we have switched the notation from B_α to B_{ij} , where $\alpha = (ij)$ is the unique microbe in our pool capable of growing on c_i and n_j . Having considered this simpler situation we will return to the most general case of unequal numbers of carbon (K) and nitrogen (M) resources and any number of microbes from a pool of S species competing for a given pair of resources.

This is where we need to revise in certain ways the network representation of a steady state used in the main text (see Fig. 1A). In the marriage game related theory, the notion of (stable or unstable) matching explicitly refers to a bipartite graph with two distinct sets of vertices and edges arranged in such a way that each one may join only a pair of elements belonging to different sets. In our case, it is natural to consider two sets of resource nodes (vertices), one including all carbon nodes and the other one containing all nitrogen nodes. An edge, or link, will appear between a carbon c_i and nitrogen n_j node if the microbe B_{ij} using these two nutrients is present in the state represented by this particular bipartite network.

Furthermore, the specifics of our version of “marriage game”, or rather “residents vs hospitals”, problem requires us to consider *directed* bipartite graphs as the steady state representations in our model. For any species B_{ij} present in a given state, we choose the direction of the edge joining node c_i with node n_j to be pointing from c_i to n_j if the microbe is limited by its carbon nutrient (and the other way around, from n_j to c_i , on the case of B_{ij} being nitrogen-limited). Fig. S1 A shows the directed bipartite graph representation of the state #5 of a particular example of $2C \times 2N \times 4S$ system considered in the “Results” section of the main text.

In what follows we will refer to a resource as *occupied* if in a given steady state there is a microbe for which this resource is rate-limiting. In our bipartite network representation occupied resources have an outgoing edge (their out-degree is equal to 1), while unoccupied resources have out-degree equal to 0.

Review of results about stable matchings in the hospitals/residents problem

The hospitals/residents problem²⁹ is known in various settings. The one directly relevant to our problem is the following. There are L applicants for residency positions in $H \leq L$ hospitals. A hospital number i has V_i vacancies

for residents to fill, V_i ranging from zero to L , $\sum V_i = L$. Each hospital has a list of preferences in which residency applicants are strictly ordered by their ranks, from 1 (the most desirable) to L , (the least desirable). These lists are generally different for different hospitals. Each applicant has a ranked list of preferred hospitals ranging from 1 (the most desirable) to H (the least desirable). Those lists can also vary between applicants. A *matching* is an assignment of applicants to hospitals such that all applicants got residency and all hospital vacancies are filled. A matching is *unstable* if there is at least one applicant a and hospital h to which a is not assigned such that:

1. Condition 1. Applicant a prefers hospital h to his/her assigned hospital;
2. Condition 2. Hospital h prefers applicant a to at least one of its assigned applicants.

If such a pair (a, h) exists, it is called “a blocking pair” or “a pair that blocks the matching”. A *stable* matching by definition has no blocking pairs. Gale and Shapley proved that for any set of applicant/hospital rankings and hospital vacancies there is at least one stable matching²⁹. Generally the number of stable matching is larger than one. For example, for stable marriages and random rankings the average number of stable matchings is given by $L/e \log L$ ³⁰. To the best of our knowledge, the dependence of this number on the distribution of hospital vacancies has not been investigated. The fact that the actual number of uninvadable states is rather close to its lower bound (compare black symbols and dashed line in Fig. 1) indicates that, at least for $L \leq 9$, the number of stable matchings averaged over all possible in-degree allocations is rather close to 1.

Gale and Shapley not only proved the existence of at least one stable matching, but also proposed a constructive algorithm on how to find it. Listed below are the main steps in this algorithm optimized for applicants. Each applicant first submits his/her application to the hospital ranking 1 in his/her preference lists. Each hospital considers all applications it received so far and accepts all of the applicants if their number is less or equal than hospital’s announced number of vacancies, L_i . If the number of applicants exceeds L_i , the hospital gives a conditional admission to the best-ranking L_i applicants according to hospital’s own preference list. Each applicant not admitted to their top hospital goes a step down on his/her preference list and applies to the second-best hospital. The latter admits this applicant if (1) this hospital has not yet filled all of its vacancies or (2) all vacancies are filled, but among the conditionally admitted applicants there is at least one who ranks lower (according to hospital’s list) than the new applicant. Such lower-ranked applicants are declined admission and replaced with better ones. They subsequently lower their expectations and apply to the next hospital on their list. After a number of iterations all applicants are admitted and all vacancies

are filled so that this process stops. As Gale and Shapley proved in Ref.²⁹, the resulting matching is stable. Furthermore, the theorem states that in this matching every applicant gets admitted to the best hospital among all stable matchings, while every hospital gets the worst set of residents among all stable matchings. Later research described in Ref.³⁰ describe more complex constructive algorithms allowing one to efficiently find all of the stable matchings starting with the applicant-optimal one.

Well developed mathematical apparatus of stable matching problem provides an invaluable help in the task of identifying all uninvadable states in microbial ecosystems. Indeed, without its assistance this task would require exponentially long time. To connect the problem of finding all uninvadable states to that of finding all stable matchings between hospitals and residents, we start with the following three observations:

1) In any uninvadable steady state, either all carbon sources or all nitrogen sources (or both) are occupied. Indeed, if in a steady state a carbon source c_i and a nitrogen source n_j are not-limiting to any microbes, then microbe B_{ij} can always grow and thereby invade this state. Thus uninvadable states can be counted separately: one first counts the states where all nitrogen sources are occupied, and then counts those in which all carbon sources are occupied. Double counting happens when both carbon and all nitrogen sources are occupied. We will keep the possibility of double counting in mind and return to this problem later.

2) For a pool of species, where for every pair of resources there is exactly one microbe using each (carbon, nitrogen) pair, one can think of each of L carbon (alternatively, nitrogen) sources as if it had a list of “preferences” ranking all nitrogen (correspondingly carbon) sources. Indeed, the ranking of competitive abilities $\lambda_{ik}^{(c)}$ of different microbes using the same carbon source c_i but different nitrogen sources n_k can be viewed as the ranking of nitrogen sources k by the carbon source i . Conversely, the ranking of $\lambda_{mj}^{(n)}$ with the same n_j but variable c_m can be thought of as ranking of carbon sources c_m by the nitrogen source n_j .

3) Consider a steady state in which all nitrogen sources are occupied. In our network representation it corresponds to every nitrogen source sending an outgoing link to some carbon source. Let L_i be the number of microbes using the carbon source i in a non-limiting fashion (the in-degree of these outgoing links ending on c_i , see Fig. S1C). Then, obviously, $L = \sum L_i$ (note that some of the terms in this sum might be equal to zero).

One can prove that if the state is uninvadable, then the matching given by all edges going from nitrogen sources to carbon sources must be stable in the Gale-Shapley sense. To prove this, let’s think of nitrogen sources as “applicants” and carbon sources as “hospitals” with their numbers of “vacancies” given by L_i . Indeed, any unstable matching has at least one blocking pair (n_j, c_i) such that:

- Condition 1. The nitrogen source (‘applicant’) n_j

“prefers” the carbon source (“hospital”) c_i to its currently assigned carbon source (the one used by the current microbe B_{kj} limited n_j). This means that $\lambda_{ij}^{(n)} > \lambda_{kj}^{(n)}$. Thus the microbe B_{ij} can grow on its nitrogen source (provided that it can also grow on its carbon source).

- Condition 2. The carbon source (“hospital”) c_i “prefers” the nitrogen source (“applicant”) n_j to at least one of L_i of its currently assigned carbon sources (the set of microbes using c_i in a non-rate-limiting fashion). Thereby $\lambda_{ij}^{(c)}$ must be larger than the smallest $\lambda^{(c)}$ among these microbes. According to the Exclusion Rule 2, this smallest $\lambda^{(c)}$ is still larger than $\lambda^{(c)}$ of the microbe limited by c_i (if it exists). Thus the microbe B_{ij} can also grow on its carbon source.

This proves that the microbe B_{ij} corresponding to any blocking pair can grow on both its carbon and its nitrogen sources, and thereby can successfully invade the steady state. This finishes the proof that any uninhabitable state has to be a stable matching in the Gale-Shapley sense.

However, this does not prove that any stable matching corresponds to exactly one uninhabitable state. To prove this we first notice that, up to this point, our candidate uninhabitable state contained only the nitrogen-limited species (See Fig. S1 B). We will now supplement it with carbon-limited species in such a way that 1) added species do not violate the exclusion rule 2; 2) added species render the state completely uninhabitable. Let us introduce a new notation (applicable to our case in which all nitrogen sources are occupied). Let $\lambda_{\min}^{(c)}(i)$ denote the smallest $\lambda^{(c)}$ among all species using c_i in a non-rate-limiting fashion. The Gale-Shapley theorem only guarantees the protection of our state from invasion by a species (i, j) with $\lambda_{ij}^{(c)}$ larger than $\lambda_{\min}^{(c)}(i)$ (see the Condition 2 above). To ensure that our state is uninhabitable by the rest of the species, one needs to add some carbon-limited species to this state. In order to do this in a systematic way, for each c_i we compile the list of all species using this carbon source with $\lambda^{(c)} < \lambda_{\min}^{(c)}(i)$. Each of these species is a potential invader. Some species could be crossed off from the list of potential invaders because they cannot grow on their nitrogen source. These species have $\lambda^{(n)}$ below that of the (unique) species limited by their nitrogen source. Among the species that remained on the list of invaders after this procedure, we select that with the largest $\lambda^{(c)}$ and add it to our steady state as a $C \rightarrow N$ directed edge, that is to say, as a carbon-limited species. This will prevent all other potential invaders on our list, since they have smaller $\lambda_{(c)}$ and thus, following the addition of our top carbon-limited species, they would no longer be able to grow based on their carbon source. We will go over all c_i and add such carbon-limited species if they are needed. The only scenario when such species is not needed if our list of potential invaders would turn up to be empty. In this case

we will leave this carbon source unoccupied. See Fig. S1 C for the illustration of an uninhabitable state constructed by the above procedure in $6C \times 6N \times 36S$ model. Since for each carbon source the above algorithm selects the carbon-limited species (or selects to add no such species) in a unique fashion, there is a single uninhabitable state for every stable matching in the Gale-Shapley sense. We are now in a position to predict and enumerate all uninhabitable states in our model.

Lower bound on the number of uninhabitable states

To count the number of partitions (L_1, L_2, \dots, L_L) such that $\sum L_i = L$, one can use a well known combinatorial method. According to this method, one introduces $L - 1$ identical “separators” (marked with $|$) which are placed between L identical objects (marked \cdot) separating them into L (possibly empty) partitions. For example, for $L = 4$ a partition $0, 1, 0, 3$ would be denoted as $|\cdot||\cdot\cdot\cdot$. The combinatorial number of all possible arrangements of separators and objects is obviously $\binom{2L-1}{L}$. For every such partition the Gale-Shapley theorem guarantees at least one stable matching (that is, at least one uninhabitable steady state). The lower bound on the number of uninhabitable steady states has to be doubled to account for reversal of roles of carbons and nitrogens. There is a small possibility that we double counted one partition $(1, 1, \dots, 1)$. Indeed, the unique uninhabitable stable state corresponding to this partition could in principle be counted both when we start from nitrogen sources and when we start from carbon sources. This could happen only when the numbers of carbon and nitrogen sources are equal to each other. More restrictively, this partition will be double-counted only if, when we started from C, all of the N-sources will send a link back to C, and these links all will end on different C-sources. The same has to be true if one starts with N-sources and then sends links back to C. The steady state network in this case will consist of one or more loops covering all nutrients. However, one can prove that, at least for the Gale-Shapley nitrogen-optimal state, the last carbon to be picked up would not need to send back a carbon-limited link. Thus in our task of calculating the lower bound on the number of uninhabitable states, we don’t need to correct for the possibility of double-counting since at least one stable matching per partition (namely the Gale-Shapley) would not be double-counted. Then we have $N_{UIS} \geq 2 \binom{2L-1}{L} = \binom{2L}{L}$. The Sterling approximation for this expression is $2^{2L}/\sqrt{\pi L}$. Thus the overall lower bound for the number of uninhabitable stable states is given by

$$N_{UIS}(L, L) \geq \binom{2L}{L} \simeq \frac{2^{2L}}{\sqrt{\pi L}} \quad . \quad (S4)$$

More generally, the number of carbon sources, K , is not equal to the number of nitrogen sources, M . The resource type with a larger number will always have at

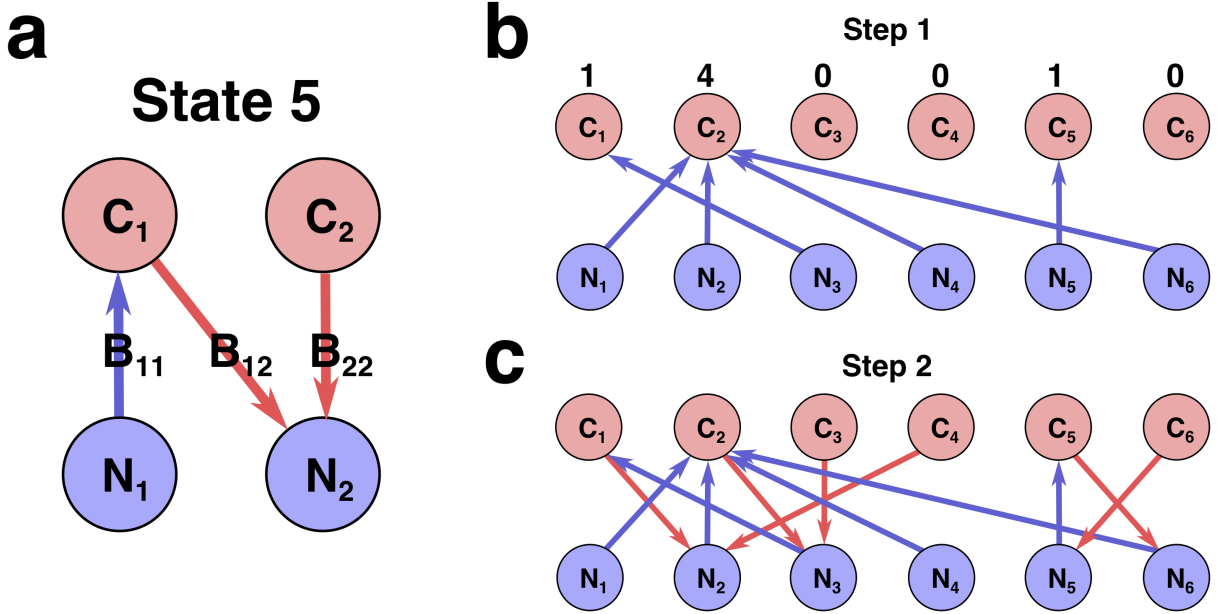


FIG. S1. **Network representation of a state in Stable Marriage analogy.** (a) Schematic representation of state #5 in the $2C \times 2N \times 4S$ model (the same state is shown in Fig. 1A in Main text). Here each species represented as an arrow connecting two resources it is utilizing for growth, with the color and direction of arrow representing growth-limitation of a species (red corresponds to C-limited species, blue N-limited one). (b)-(c) Schematic representation of two-step construction of state #991 in the $6C \times 6N \times 36S$ model. (b) We first assign all species that are growth-limited by N (blue links outgoing from N sources). The numbers above C sources indicate number of vacancies for a given resource. (c) Then for a given set of N-limited species we populate the remaining C-limited ones that are allowed by the Condition 2 (red links outgoing from C sources).

least one resource left without input. Thus here one never needs to correct for double counting. Using the same reasoning as for $K = M = L$, the lower bound on the number of resources in this case is given by $\binom{K+M-1}{K-1} + \binom{K+M-1}{M-1} = \binom{K+M}{K}$. Here, the first term counts the uninhabitable steady states in which all nitrogen sources are occupied and the partition divides M edges sent by nitrogen sources among K carbon sources, which requires $K - 1$ “dividers”. The second term counts the number of uninhabitable steady states in which all carbon sources are occupied. Denoting the fraction of carbon resources among all resources as $p = K/(K + M)$ and using the Stirling approximation one gets

$$N_{UIS}(K, M) \geq \binom{K+M}{K} \simeq \frac{\exp[(K+M)(-p \log p - (1-p) \log(1-p))]}{\sqrt{2\pi(K+M)p(1-p)}}. \quad (\text{S5})$$

In the case of multiple microbial species using the same pairs of resources, our version of the Gale-Shapley resident-oriented algorithm must be further updated. Let M be the number of nitrogen sources, and K — the number of carbon sources in the ecosystem, S the number of species in our pool, each requiring a pair of resources to grow. As now there may be more than one microbe that uses a given pair of resources c_i and n_j , we introduce the notation $B_{ij}^{(r)}$ for the r th microbe using the same pair of

sources c_i and n_j . On average, each nitrogen (carbon) source has S/K (S/M) microbes, which are capable of using it. As in the traditional Gale-Shapley algorithm, each nitrogen (carbon) source ranks all microbes capable of using it by their $\lambda^{(n)}$ ($\lambda^{(c)}$).

The way to identify all uninhabitable stable states in this case is determined by a variant of the stable marriage problem (or rather the hospital/resident problem) in which every man (and every woman) may have more than one way to propose marriage to the same woman (man). In our model this corresponds to more than one microbe (a type of marriage) capable of growing on the same pair of carbon (corresponding to, say, men) and nitrogen (corresponding to women) sources. You may think of it as if each participant has several different ways to propose to the person of the opposite sex (send flowers, take to a restaurant, etc). Each of these proposals is ranked by both parties independent of other ways. As far as we know, this variant has not been considered in the literature yet. However, all of the results of the usual stable marriage (or hospital-resident) problem remain unchanged.

One can easily see that our lower bound (Eq. S5) on the number of uninhabitable states (equal to the number of stable marriages in all partitions) remains unchanged. Indeed, it is given by the number of partitions and hence depends only on K and M and not on S . However, for

$S \gg K \cdot M$ one expects to have many more stable marriages for each partition. Thus the lower bound we have established is likely to severely underestimate the actual number of UIS in the ecosystem.

D. Conditions of multistability in the $2C \times 2N \times 4S$ ecosystem

Below we consider the general case of a $2C \times 2N \times 4S$ ecosystem. Let's assume that the selected set of λ parameters allow potentially unstable state in which all four species are present. These species form a single loop in the network representation (like state S7 in our 2Cx2Nx4S example). Without loss of generality we may assume that λ -parameters satisfy $\lambda_{11}^{(n)} > \lambda_{21}^{(n)}$; $\lambda_{21}^{(c)} > \lambda_{22}^{(c)}$; $\lambda_{22}^{(n)} > \lambda_{12}^{(n)}$; $\lambda_{12}^{(c)} > \lambda_{11}^{(c)}$. The 4-species loop is then formed by the links $C_1 \rightarrow N_1$, $N_1 \rightarrow C_2$, $C_2 \rightarrow N_2$, and $N_2 \rightarrow C_2$. In all other cases we may rename C and N resources until the direction of the loop is as stated above. The system also has two uninvadable steady states (A) in which two microbes ($N_1 \rightarrow C_1$ and $N_2 \rightarrow C_1$) are limited by their nitrogen sources and (B) in which two other microbes are limited by their carbon sources ($C_1 \rightarrow N_2$ and $C_2 \rightarrow N_1$). These two states have their regions of feasibility in the influx space. In order for these regions to overlap with each other, thereby resulting in bistability within the overlapping region, the yield parameters of species and nutrient supply rates have to satisfy the following conditions.

For the state (A), the conservation laws read as

$$\begin{aligned} \frac{\Phi_1^{(c)}}{\delta} &= c_1 + \frac{B_{11}}{Y_{11}^{(c)}} \\ \frac{\Phi_2^{(c)}}{\delta} &= c_2 + \frac{B_{22}}{Y_{22}^{(c)}} \\ \frac{\Phi_1^{(n)}}{\delta} &= \frac{\delta}{\lambda_{11}^{(n)}} + \frac{B_{11}}{Y_{11}^{(n)}} \\ \frac{\Phi_2^{(n)}}{\delta} &= \frac{\delta}{\lambda_{22}^{(n)}} + \frac{B_{22}}{Y_{22}^{(n)}} \end{aligned} \quad (\text{S6})$$

The last two relations in (Eq. S6) define microbe concentrations as $B_{11} = \frac{Y_{11}^{(n)}}{Y_{11}^{(c)}} \left(\frac{\Phi_1^{(n)}}{\delta} - \frac{\delta}{\lambda_{11}^{(n)}} \right)$, $B_{22} = \frac{Y_{22}^{(n)}}{Y_{22}^{(c)}} \left(\frac{\Phi_2^{(n)}}{\delta} - \frac{\delta}{\lambda_{22}^{(n)}} \right)$. Substituting these expressions into the first two relations in (Eq. S6) and invoking the requirements $c_1 > \frac{\delta}{\lambda_{11}^{(c)}}$, $c_2 > \frac{\delta}{\lambda_{22}^{(c)}}$ (guaranteeing that neither of two carbons limits microbes' growth), in the high

flux limit we obtain

$$Y_{11}^{(n)} \Phi_1^{(n)} < Y_{11}^{(c)} \Phi_1^{(c)} \quad (\text{S7})$$

$$Y_{22}^{(n)} \Phi_2^{(n)} < Y_{22}^{(c)} \Phi_2^{(c)}$$

The inequality conditions above are only natural given that the microbes use up their nitrogen fluxes very thoroughly in the state (A) while (at least in the high-flux limit) they not getting even close to consuming all of their carbon supply rates.

The state (B) in the high flux limit will require different conditions, though obtained in a perfectly similar way:

$$Y_{12}^{(n)} \Phi_2^{(n)} > Y_{12}^{(c)} \Phi_1^{(c)} \quad (\text{S8})$$

$$Y_{21}^{(n)} \Phi_1^{(n)} > Y_{21}^{(c)} \Phi_2^{(c)}$$

Combining Eq. S7 and Eq. S8 one gets

$$\frac{Y_{11}^{(c)}}{Y_{11}^{(n)}} \Phi_1^{(c)} > \Phi_1^{(n)} > \frac{Y_{21}^{(c)}}{Y_{21}^{(n)}} \Phi_2^{(c)} \quad (\text{S9})$$

$$\frac{Y_{22}^{(c)}}{Y_{22}^{(n)}} \Phi_2^{(c)} > \Phi_2^{(n)} > \frac{Y_{12}^{(c)}}{Y_{12}^{(n)}} \Phi_1^{(c)}$$

Hence, for the carbon fluxes ratio, one would have

$$\frac{Y_{21}^{(c)} Y_{11}^{(n)}}{Y_{21}^{(n)} Y_{11}^{(c)}} < \frac{\Phi_1^{(c)}}{\Phi_2^{(c)}} < \frac{Y_{22}^{(c)} Y_{12}^{(n)}}{Y_{22}^{(n)} Y_{12}^{(c)}} \quad (\text{S10})$$

which implies that for multistability to be possible at least for some ration of fluxes the yields have to satisfy the following inequality:

$$\frac{Y_{21}^{(c)} Y_{11}^{(n)} Y_{22}^{(n)} Y_{12}^{(c)}}{Y_{21}^{(n)} Y_{11}^{(c)} Y_{22}^{(c)} Y_{12}^{(n)}} < 1 \quad (\text{S11})$$

Note that the Eq. S11 is both necessary and sufficient for bistability between (A) and (B) for some set of supply rates. Indeed, if Eq. S11 is satisfied, $\Phi_2^{(c)}$ can be chosen arbitrarily (the only thing one would have to mind here is the high-flux limit requirements), then $\Phi_1^{(c)}$ should be chosen in accordance with Eq. S10, and any nitrogen fluxes satisfying Eq. S9. All the procedures are legitimate whenever Eq. S11 holds. Once chosen in the way described above, the point $(\Phi_1^{(c)}, \Phi_2^{(c)}, \Phi_1^{(n)}, \Phi_2^{(n)})$ of the influx space will make both (A) and (B) steady states feasible.

In a more general case of an arbitrary number of nutrients of each type, the conditions allowing for bistability or even multistability can be expressed by simple inequalities connecting yields and fluxes in combinations dictated by network topology of potentially bistable states in a very similar way to the simple case presented above. Thus the solution to the puzzle of why roughly

half of all possible yield combinations has no multistability whatsoever becomes intuitively clear. Indeed, these yields and fluxes must come in “dimensionless” combinations so that any inequality can be written as a function

of only C:N stoichiometry $S_{ij}^{(C:N)} = \frac{Y_{ij}^{(n)}}{Y_{ij}^{(c)}}$ for all micro-

bial species present in any of the set of potentially multistable states. Note that **should nitrogen and carbon yields exchange places for each of these microbes, the key inequality similar to Eq. S11 would be reversed**, thus prohibiting multistability where it was permitted and vice versa.

In the yield space, the proposed swap of carbon and nitrogen yields of all species $Y^{(c)} \rightarrow Y^{(n)}$, $Y^{(n)} \rightarrow Y^{(c)}$ is a volume preserving transformation. This means that, for each set of potentially multistable states, the fraction of the yield space favouring multistability is exactly the same as the fraction prohibiting multistability. In a possible (albeit unlikely) scenario when the suggested permutation affects not only the potential multistability in question, but also some other multistable conditions, “turning off” one multistability might in some cases “turn on” others. This is why the ultimate empirical probability of multistability for a given combination of species’ yields might somewhat deviate from 1/2.

VII. SUPPLEMENTARY TABLES

TABLE I. $\lambda_{i,j}^c, \lambda_{i,j}^n$ values of the 4 species for the 2Cx2Nx4S model.

| | $\lambda_{i,j}^c$ | | $\lambda_{i,j}^n$ | |
|-------|-------------------|-------|-------------------|-------|
| | n_1 | n_2 | n_1 | n_2 |
| c_1 | 41 | 35 | 16 | 50 |
| c_2 | 52 | 56 | 27 | 44 |

TABLE II. Values of carbon and nitrogen Yields of the 4 species for the 2Cx2Nx4S model.

| | $Y_{i,j}^c$ | | $Y_{i,j}^n$ | |
|-------|-------------|-------|-------------|-------|
| | n_1 | n_2 | n_1 | n_2 |
| c_1 | 0.37 | 0.64 | 0.27 | 0.10 |
| c_2 | 0.47 | 0.14 | 0.22 | 0.59 |

TABLE III. $\lambda_{(i,j)}^{(c)}$ values of the 36 species for the 6Cx6Nx36S model.

| | N_1 | N_2 | N_3 | N_4 | N_5 | N_6 |
|-------|-------|-------|-------|-------|-------|-------|
| C_1 | 47.4 | 78.1 | 93.7 | 68.9 | 75.0 | 44.5 |
| C_2 | 89.6 | 68.6 | 33.6 | 77.8 | 16.5 | 90.8 |
| C_3 | 56.5 | 32.2 | 86.2 | 13.1 | 71.1 | 15.5 |
| C_4 | 53.0 | 94.1 | 38.7 | 10.7 | 34.0 | 34.9 |
| C_5 | 25.0 | 49.3 | 76.3 | 18.2 | 54.5 | 51.8 |
| C_6 | 47.1 | 91.9 | 57.7 | 63.0 | 92.2 | 90.0 |

TABLE IV. $\lambda_{(i,j)}^{(n)}$ values of the 36 species for the 6Cx6Nx36S model.

| | N_1 | N_2 | N_3 | N_4 | N_5 | N_6 |
|-------|-------|-------|-------|-------|-------|-------|
| C_1 | 18.3 | 57.7 | 44.5 | 16.0 | 70.4 | 66.8 |
| C_2 | 56.7 | 31.4 | 78.6 | 91.8 | 34.5 | 34.7 |
| C_3 | 42.3 | 53.8 | 84.8 | 99.2 | 79.0 | 44.6 |
| C_4 | 95.3 | 91.4 | 73.1 | 42.9 | 98.8 | 66.7 |
| C_5 | 76.2 | 98.4 | 31.0 | 55.4 | 14.5 | 57.4 |
| C_6 | 37.6 | 79.3 | 58.4 | 71.8 | 26.0 | 84.5 |

TABLE V. $Y_{(i,j)}^{(e)}$ values of the 36 species for the 6Cx6Nx36S model.

| | N_1 | N_2 | N_3 | N_4 | N_5 | N_6 |
|-------|-------|-------|-------|-------|-------|-------|
| C_1 | 0.72 | 0.59 | 0.15 | 0.11 | 0.13 | 0.75 |
| C_2 | 0.29 | 0.72 | 0.79 | 0.39 | 0.15 | 0.16 |
| C_3 | 0.76 | 0.61 | 0.40 | 0.86 | 0.60 | 0.63 |
| C_4 | 0.87 | 0.68 | 0.64 | 0.27 | 0.80 | 0.51 |
| C_5 | 0.88 | 0.13 | 0.31 | 0.36 | 0.11 | 0.48 |
| C_6 | 0.46 | 0.34 | 0.38 | 0.83 | 0.70 | 0.86 |

TABLE VI. $Y_{(i,j)}^{(n)}$ values of the 36 species for the 6Cx6Nx36S model.

| | N_1 | N_2 | N_3 | N_4 | N_5 | N_6 |
|-------|-------|-------|-------|-------|-------|-------|
| C_1 | 0.10 | 0.30 | 0.67 | 0.36 | 0.32 | 0.66 |
| C_2 | 0.83 | 0.30 | 0.47 | 0.30 | 0.40 | 0.58 |
| C_3 | 0.72 | 0.15 | 0.65 | 0.54 | 0.21 | 0.18 |
| C_4 | 0.30 | 0.22 | 0.84 | 0.64 | 0.29 | 0.56 |
| C_5 | 0.55 | 0.16 | 0.77 | 0.42 | 0.22 | 0.25 |
| C_6 | 0.49 | 0.67 | 0.89 | 0.80 | 0.50 | 0.19 |

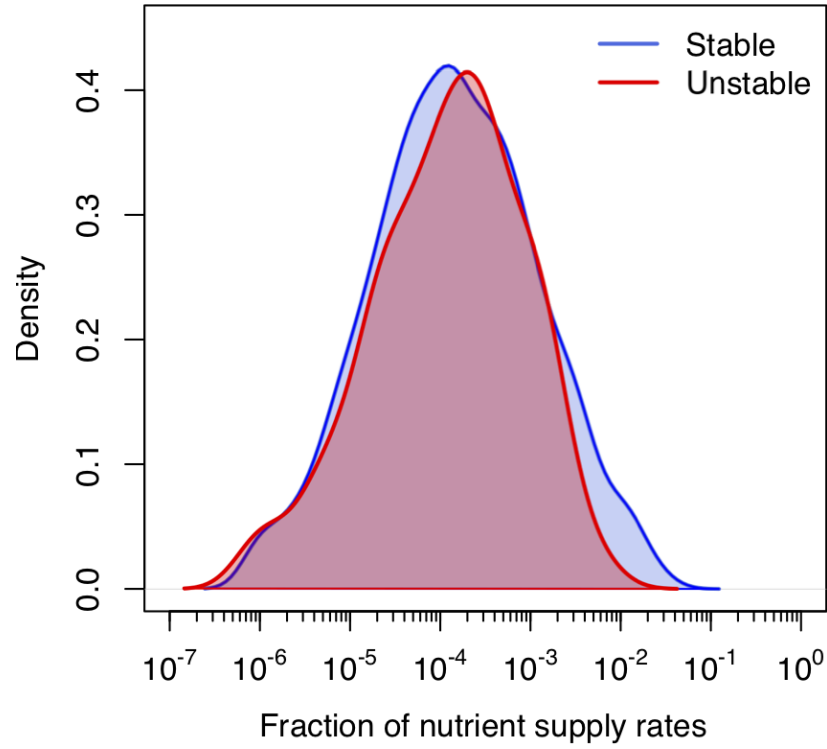


FIG. S2. **Distribution of volumes for stable and unstable states.** Log-normal distribution of feasible volumes of 1211 uninvadable states in $6C \times 6N \times 36S$ version of our model. Red line is used for 1058 dynamically stable states and blue line for 153 dynamically unstable ones. Distributions are normalized to the total number of states of each type. The natural logarithm of the volume has mean $\mu = -8.87 \pm 0.06$ and standard deviation $\sigma = 2.08 \pm 0.04$. There is no significant difference between distributions of volumes of stable and unstable uninvadable states (two-sample Kolmogorov-Smirnov test: p-value= 0.94).

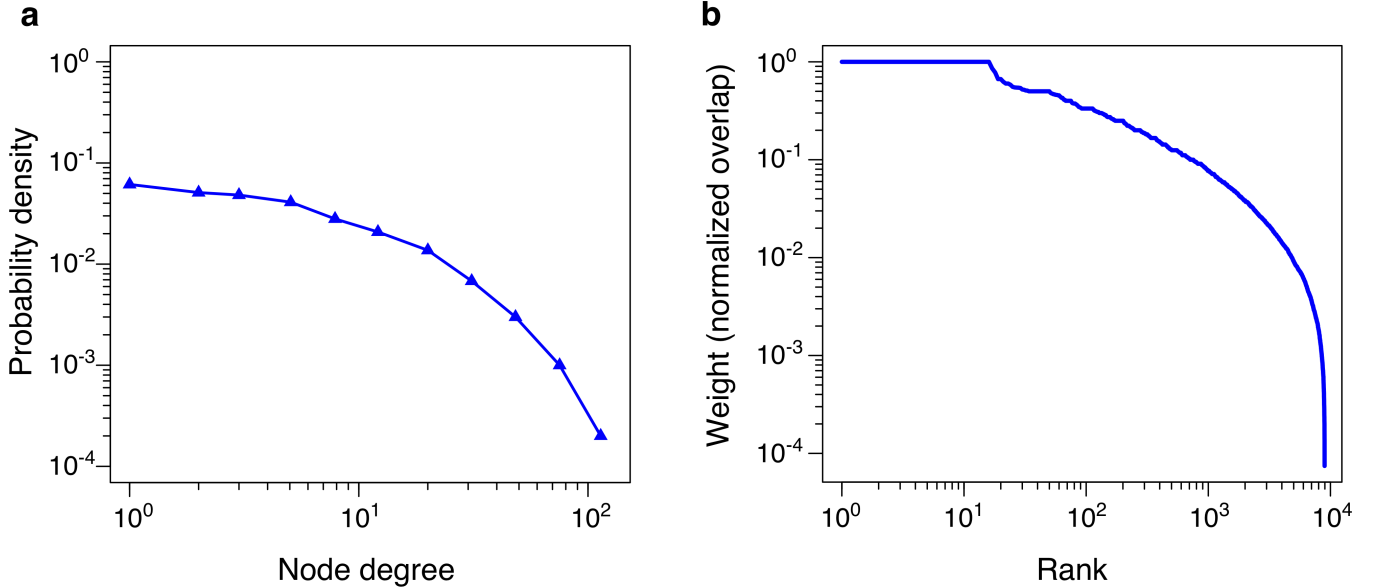


FIG. S3. **Statistics of pairwise bistability network for $6C \times 6N \times 36S$ example.** (a) Degree distribution of the network in Fig. 2F. (b) Rank-ordered distribution of weights of network edges from Fig. 2F. The weights of the network in Fig. 2F are given by normalized overlaps between states.

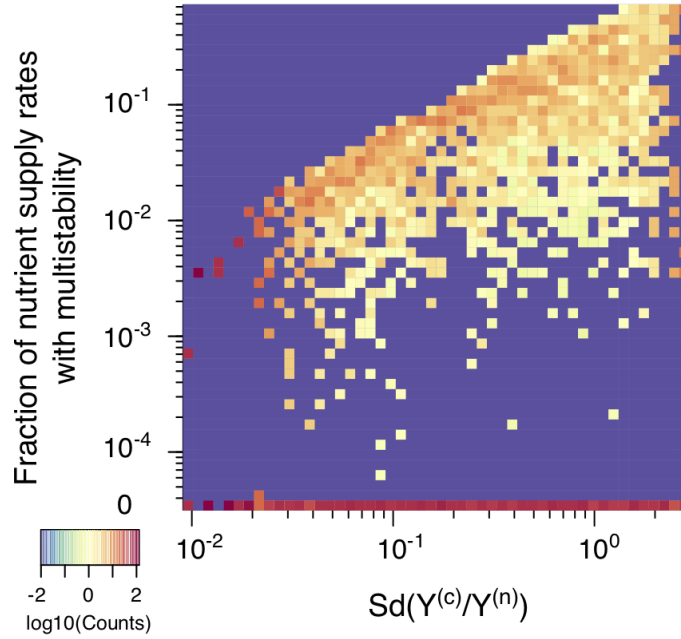


FIG. S4. **Statistics of multistability for different combinations of yields.** Heatmap of the fraction of nutrient supply rate combinations that permit multistability for the $2C \times 2N \times 4S$ model with diverse combinations of microbial growth yields (4000 model variants in total) with diverse values of microbial growth yields. The color scale represents \log_{10} of normalized counts of examples for a given interval of standard deviation of yields (X-axis) and the fraction of nutrient supply rates with multistability (Y-axis). The bottom row (0) corresponds to 2069 yields combinations where no multistability was observed.

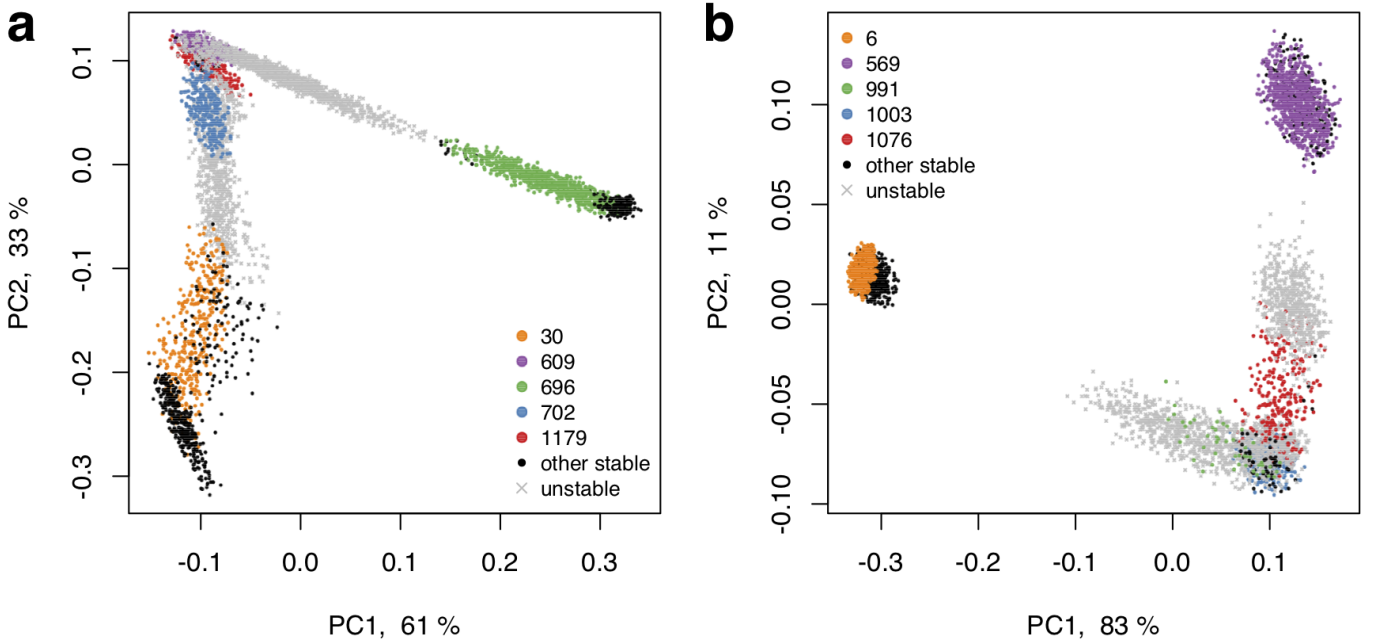


FIG. S5. **The PCA plot of fractional microbial abundances.** These abundances, normalized to 1, were obtained in our simulations for supply rates in the local vicinity of a multistable point where $V = 5$ stable states coexist. Panels (a) and (b) represent the two remaining multistable points in addition to the multistable point shown in Fig. 3C. Axes show the percentage of the variance explained by each principle component. Each point show the first (x-axis) and the second (y-axis) principal coordinates of microbial abundances in an uninvadable state feasible for a given set of nutrient supply rates. The supply rates were chosen to be close ($\pm 10\%$) to the initial multistable point. Colored circles mark the original five stable states, black circles - other stable states which became feasible for nearby supply rates, and grey crosses - dynamically unstable states feasible in this influx region. Note a quasi-1D manifold along which the points of all colors are aligned and the alternating order of points corresponding to stable and unstable states.